

University of Nevada, Reno

**KSHV encoded viral processivity factor, ORF59, regulates multiple pathways for
viral replication**

A thesis submitted in partial fulfillment of the requirements for the degree of Master of
Science in Cellular and Molecular Biology

by

Kammi L. Dingman

Dr. Subhash Verma/Thesis Advisor

December, 2017



THE GRADUATE SCHOOL

We recommend that the thesis
prepared under our supervision by

KAMMI L. DINGMAN

Entitled

**KSHV Encoded Viral Processivity Factor, ORF59, Regulates Multiple Pathways
For Viral Replication**

be accepted in partial fulfillment of the
requirements for the degree of

MASTER OF SCIENCE

Subhash C. Verma, Ph.D., Advisor

Cyprian C. Rossetto, Ph.D., Committee Member

Patricia M. Berninsone, Ph.D., Graduate School Representative

David W. Zeh, Ph.D., Dean, Graduate School

December, 2017

ABSTRACT

Kaposi's Sarcoma-Associated Herpesvirus (KSHV), or human herpesvirus 8 (HHV-8), is a tumorigenic herpesvirus tightly linked with various human malignancies including Kaposi's Sarcoma, Primary Effusion Lymphomas (PELs), and Multicentric Castleman's Disease (1). Immunocompetent individuals infected with KSHV are asymptomatic, but the immunocompromised individuals are at risk for developing cancers (2). ORF59, a DNA processivity factor of the viral DNA polymerase, is essential for lytic reactivation and is highly expressed during de novo primary infection. To better understand the role of ORF59, we performed an ORF59-immunoprecipitation from KSHV infected cells and identified ORF59 interacting proteins through protein sequencing and LC/MS spectrometry analysis. From a large number of ORF59 interacting proteins, we selected few candidates for further study, which includes host proteins Nucleolin and MCM4, in addition to viral protein, ORF57. Our characterization of the interaction between KSHV ORF59 and these associating factors yielded exciting new insights on host-virus interactions that we believe to be valuable for understanding KSHV pathogenesis. Nucleolin (NCL), involved in ribosome assembly, pre-mRNA metabolism, cytoplasmic RNA stability, and nucleo-cytoplasmic transport as well as ORF57, an mRNA transcript accumulation (MTA) viral early protein involved in posttranscriptional regulation, splicing of viral RNA transcripts, RNA stability, and transcriptional activation, bound specifically to ORF59. ORF59 also associated with minichromosome maintenance proteins (MCMs), a complex of DNA replication licensing factor required for cellular DNA replication.

DEDICATION

This thesis is dedicated to my beloved parents, Tammi and Manuel Moniz. They are everything and more than a daughter could ask for. There are no words to express my love and gratitude.

ACKNOWLEDGEMENTS

We thank Dr. Britt Glaunsinger, University of California at Berkley for providing cDNA clones of Nucleolin. Thanks to Dr. Vladimir Majerciak from the NIH for the ORF57 expression vectors.

TABLE OF CONTENTS

	Pages
Introduction	1
Materials and Methods	11
Results	18
Discussion	34
Future Directions	39
References	41

List of Tables

- List of primers used in this study

List of Figures

ORF59

- Schematic illustrating the ORF59-GFP and Myc epitope tagged segments used for binding assays.

NCL

- ORF59 associates with Nucleolin
- ORF59 and Nucleolin colocalizes during lytic reactivation

ORF57

- ORF59 and ORF57 associates endogenously
- ORF59 and ORF57 proteins associate directly
- ORF59 1-264 aa associates with ORF57
- ORF59 segment 2 subsegments associate with ORF57 in an overexpression system.

MCM4

- ORF59 segments associate with MCM4 in an overexpression system
- ORF59 segment 2 subsegments associate with MCM4 in an overexpression system
- ORF59 and MCM4 colocalizes during lytic reactivation

INTRODUCTION:

Herpesviruses are large, double-stranded DNA (dsDNA) viruses that replicate in the nuclei of the infected host cell. Based on biological characteristics and genomic organization, herpesviruses are divided into subfamilies: Alphaherpesvirinae (α), Betaherpesvirinae (β), and Gammaherpesvirinae (γ) (3, 4). Gammaherpesviruses are further classified into two groups, Lymphocryptoviruses and Rhadinoviruses. The *Lymphocryptovirus* (gamma-1) genus includes: Epstein-Barr virus (EBV) and Herpesvirus papio. The *Rhadinovirus* (gamma-2) genus includes following species: Herpesvirus saimiri (HVS), Kaposi's sarcoma-associated herpesvirus (KSHV), Rhesus rhadinovirus (RRV), Equine herpesvirus 2 (EHV-2), and Murine gammaherpesvirus-68 (MHV-68). All gammaherpesviruses have the ability to induce abnormal growth of cells (neoplasia) in experimental and natural hosts (5).

Kaposi's Sarcoma-Associated Herpesvirus (KSHV), also known as human herpesvirus 8 (HHV-8), is a large double-stranded DNA virus, which is the causative agent of Kaposi's Sarcoma (KS), Primary Effusion Lymphoma (PEL), KSHV-Inflammatory Cytokine Syndrome (KICS), and Multicentric Castleman's Disease (MCD) (1, 6, 7). The KSHV genome is approximately 165,000 nucleic acid bases in length and encodes for almost 90 open reading frames (ORFs), multiple microRNA (miRNA), and long non-coding RNAs (lnc RNAs) (8, 9). The ORFs of KSHV are named after their homology with HVS, the first Rhadinovirus characterized (9). The KSHV genome also shares high gene homology with related gammaherpesviruses (γ -1) EBV, RRV, and MHV-68 (10-13).

The linear KSHV genome is encased in an icosahedrally symmetrical capsid (spherical to pleomorphic), which is similar to the other herpesviruses capsids (14). The capsid architecture has a T=16 triangulation number shell composed of 162 capsomers (hexamers and pentamers), 4 structural proteins, heterotrimer triplexes, external protrusions, and a portal at the 12th vertex for DNA entry and exit from the capsid shell (14, 15). KSHV viral particles obtain their envelope while budding from the host cell into the luminal vesicles during viral egress (16). In between the capsid and envelope is the electron-dense connective material called the tegument layer, which has multiple viral proteins including ORFs 11, 21, 33, 45, 50, 52, 63, and 75 . The lipid envelope has conserved membrane glycoproteins on the surface that facilitates endocytosis of the virions (17).

Because of the broad range of host cells that can be infected *in vivo* (including CD19⁺ peripheral blood B cells, monocytes, endothelial cells, keratinocytes, and epithelial cells), it's not surprising that researchers have used multiple different host cells for studying KSHV biology (18). The infection of various cells is possible because KSHV uses a diverse range of host cell receptors for attachment and entry into the target cells (human and non-human cell) and is presented with different gene expression profiles (19).

Diseases or Pathogenesis

Kaposi's Sarcoma is named after the Hungarian dermatologist, Moritz Kaposi, who first characterized the specific skin sarcoma tumors he observed on patient's skin during his practice in 1872. The causative agent was unknown until formally discovered in 1994 by Patrick S. Moore and Yuan Chang lab at Columbia University (20). KSHV is

linked to sarcoma, lymphoproliferative diseases, and implicated in KICS as well as multiple myeloma (21, 22). KSHV has multiple clinical presentations including AIDS-associated Kaposi's Sarcoma, Classic/Mediterranean Kaposi's Sarcoma, Endemic/African Kaposi's Sarcoma, and Iatrogenic/Immunosuppressive Treatment-Related Kaposi's Sarcoma. Symptoms associated with infection are skin lesions, the development of internal or external tumors, discolored macules (raised blemishes or blotches), and discolored plaques and nodules .

Immunocompromised individuals that are infected with KSHV can present sarcoma lesions of the skin and oral cavity. Biopsy, Serological assay, polymerase chain reaction (PCR), and *in situ* hybridization are typically used to diagnose KSHV from the patient samples (23). Chemotherapy is often ineffective because KSHV tumors demonstrate resistance and current antivirals do not clear the virus from the host and do not adequately suppress tumorigenesis (24, 25).

Notably, if an individual is infected with KSHV prior to becoming immunocompromised, their anti-KSHV immunity is altered during immunosuppression and KSHV is prompted to lytically reactivate. While the adaptive immune system does mount a response with T-lymphocytes at the forefront along with B-lymphocytes, herpesviruses have cleverly evolved many mechanisms to escape T-cell responses (26, 27).

Vaccine or Antivirals Therapy

There are no licensed drugs or standard therapeutic practices to combat KSHV-induced malignancies as the carcinomas become resistant to chemotherapy and the antiviral therapies that target viral DNA polymerase become ineffective due to mutations

in the polymerase gene (28-33). These limitations illustrate the need for novel therapeutics that utilize new methods and fresh perspectives of the KSHV lifecycle.

Current treatments for KSHV pathologies include surgery, radiation, chemotherapy, and biological therapy. There are currently no candidate vaccines to protect from KSHV infection. Treatment of HIV infected individuals with highly active antiretroviral therapy (HAART), introduced in 1996, reduced the prevalence of AIDS associated malignancies and deaths significantly (24, 34). The use of HAART has decreased the incidence of KS by 80% (35, 36). HAART inhibition of viral reverse transcriptase blocks the HIV replication cycle; however, it does not directly block KSHV replication therefore, KS can still occur in HAART treated HIV-infected patients (37, 38). Even with the use of HAART, KS is still among the most common cancer in HIV infected individuals (25). Other treatment approaches include the use of antivirals Ganciclovir, Valganciclovir, and Phosphonoformic Acid (PFA), which are nucleoside analogs and pyrophosphate analogs that target the viral DNA polymerase activity without affecting the host DNA polymerase (32, 33). Unfortunately, KSHV is capable of evolving resistance to these antiviral drugs and not to mention these drugs are unable to clear the persistent infection from the infected host cells (28). Therefore, targeted and aggressive treatment strategies are needed, which are translatable to patients experiencing bleak virologic failure and resistance to current antivirals. Additionally, these antivirals, Gancyclovir, valganciclovir, and PFA exert side effects including fever, low level of granulocytes, decrease white blood cells (WBCs), diarrhea, nausea, headache, tremors, electrolyte disturbances, genital ulceration, and nephrotoxicity (29, 32). Moreover, the current therapies do not actually clear KSHV infection from the infected host. Since both

phases of the viral life cycle (latent and lytic phases) are involved in tumorigenesis, simply blocking lytic viral replication will not efficiently stop tumor growth.

Due to the homology of many herpesviral proteins to the host proteins, targeting drugs must have a high specificity towards the *viral* targets. Prodrugs are compounds that remain biologically inactive until metabolized by the infected cell into a drug, are used to target viral replication. More specifically, prodrugs such as acyclovir (ACV) or penciclovir (PCV) only target KSHV-infected cells because they get phosphorylated by the viral kinase (29). One advantage of developing prodrugs is an increased efficacy of targeting viral replication with reduced off-target or toxic side effects.

Geographical/Social Distribution/Seroprevalence

Approximately 15–20% of human cancers are caused by oncogenic viruses (39). KSHV is one of the seven human cancer-causing viruses. Co-infection of KSHV with HIV affects numerous people in the Mediterranean and sub-Saharan African countries. Seroprevalence varies according to geographic region; approximately 50% of people from sub-Saharan Africa, 10-25% of the Mediterranean and Middle East, and less than 10% of Northern Europe, Asia, and North Americas are KSHV infected (2).

Healthy individuals infected with the virus maintain a life-long, asymptomatic infection while immunocompromised individuals such as HIV-infected individuals, patients on immuno-suppressant drugs, and organ donation recipients are at a much higher risk of developing KSHV-associated malignancies (2). Viral coinfections that have demonstrated the ability to activate KSHV lytic replication and impact pathogenesis include: Human Immunodeficiency Virus (HIV), Herpes Simplex Virus type 1 (HSV-1), Herpes Simplex Virus type 2 (HSV-2), Human Cytomegalovirus (HCMV), Human

Herpesvirus-6 (HHV-6), Human Herpesvirus-7 (HHV-7), and Human Papillomavirus (HPV) (40-47). Additionally, inflammatory cytokine, oncostatin M, interferon- γ (IFN- γ), hepatocyte growth factor (HGF), and toll-like receptors 7 and 8 (TLR7/8) can trigger lytic reactivation (48, 49).

Not much was known about KSHV's prevalence in different populations until the emergence of HIV and symptoms of KSHV appeared in many of the HIV-infected individuals. Decline in HIV transmission led to a reduction in KS cases (50). KSHV studies analyzing genomic strain variability and seroprevalence in distinct geographic locations suggest that KSHV is a tens of thousands of years old ancient human virus (51). Another puzzling aspect of KSHV epidemiology is the fact that men appear to be infected with higher incidence than females (52, 53).

While the mode of KSHV transmission is also imperfectly understood, it has been determined that KSHV can spread by means of oral (deep kissing), blood, sexual, vertical transmission from mother to child, as well as through organ transplantation. Transmission of KSHV during organ transplantation has been detected in 1 out of every 500 cases (54). These transplant recipients either received a KSHV-infected organ or were infected with KSHV prior to transplantation.

Life Cycle

Efficient viral entry is essential for KSHV infection and consequently, pathogenesis. KSHV can enter the cells by fusing with a host cell xCT receptor, an interaction mediated by envelope glycoproteins gB and gPK8.1A, which assist in initial contact with integrin $\alpha 3\beta 1$ (17, 55). Following primary infection, the virus establishes latency in the host, which is a "dormant" condition that limits viral gene expression and

DNA replication to a bare minimum. No infectious virion particles are produced and latent DNA replication of viral genes involves restricted expression of genes from a small area of the KSHV genome that encodes proteins mandatory for the survival and propagation of the virus. Expression of these proteins ensure that dividing host daughter cells all receive copies of the viral genome to maintain a persistent infection. During this dormant stage, the viral genome exists in the form of a circularized extrachromosomal viral episome tethered to the host chromosome by latency-associated nuclear antigen (LANA/ORF73) (8, 56-58). LANA is also largely in charge of recruiting the host cellular machinery (essentially pirating host proteins) to make copies of the viral genome that gets segregated and passed into the daughter cells along with the host chromosomes (11). By restricting the expression of viral genes and utilizing cellular proteins during latency, the virus more easily evades the host's immune surveillance systems and triggering of apoptosis (59-61). Thus, LANA and other latent proteins make sure that the host cells are perpetually KSHV infected, yet keep the infection "under the radar" of host immune surveillance by holding a tight rein on lytic reactivation and by directly subverting cellular immune-sensing pathways.

The second phase of the bi-phasic lifecycle, also common to other herpesviruses, is the lytic reactivation. Various stimuli including viral co-infection and environmental factors such as hypoxia (low tissue oxygen concentration), chemical agents, and oxidative stress (due to the reactive oxygen species), can provoke the virus out of the latent phase to enter into the lytic replication phase where virion particles are produced and released (62). Lytic reactivation entails a synchronized cascade of viral gene expression leading to a mass production and discharge of infectious virion particles (6).

During this phase, cellular pathways are hi-jacked to promote viral replication and to favor virion propagation (11). One protein in particular, viral DNA replication and transcription activator (RTA/ORF50), is essential for this transition. RTA is an immediate early protein that triggers the progressive expression of immediate early, early, and late viral genes to produce infectious virions (6, 56, 58, 61, 63). RTA/ORF50 not only auto-activates its own promoter, but also the promoters of other lytic factors to essentially mobilize the recruitment of transcription factors that initiate transcription of the other viral genes (64, 65). RTA binds and activates promoters of lytic genes that contain K-RTA response elements (RREs) (66). Many transcripts/genes of the lytic phase are transactivated by RTA, which includes polyadenylated nuclear RNA, ORF59, ORF57 (MTA), vIL-6, K-bZIP, vIRF1, vOX, ORF52, ORF-K1, small viral capsid protein (ORF65), ORF56, SOX (ORF37) (21, 65, 67-79). Previous studies have shown that deletion of RTA debilitates lytic replication (80). In summary, viral RTA is both necessary and sufficient to orchestrate lytic reactivation of KSHV (81).

The major player of the latent and lytic phases, LANA and RTA, respectively, interact with one another in what is essentially a yin and yang relationship. As initiator and controller of lytic replication, RTA is the major protein responsible for latent to lytic switch (63, 82, 83). LANA has shown the ability to suppress RTA promoter and other RTA-responsive genes (84). Interaction between LANA and RTA has been observed, with LANA demonstrating the ability to inhibit RTA gene expression and auto-activation by recruiting the recombinant signal binding protein for immunoglobulin κ J region (RBP-J κ protein); RBP-J κ competes with RTA for binding to RBP-J κ (84-86). While it's clearly demonstrated that the transition from latency to lytic reactivation relies on the

regulatory activities of LANA and RTA, current research has and will continue to ascertain molecular details of this transition and the involvement of additional cellular and viral factors.

Although the two phases of the lifecycle exhibits dynamically diverse viral gene expression systems, in both stages virus modulates various cellular and viral genes to promote optimal conditions for the viral life cycle (87). While ongoing research over the past twenty years has furnished many important details concerning the molecular biology of this virus, there is yet to be a development of a cure or vaccine to protect against KSHV infection and the potential deadly consequences.

The objective of the work presented here is to furnish a greater understanding of the interaction between KSHV viral proteins with host's counterparts during lytic reactivation. By developing a clear understanding of how cellular proteins are manipulated by KSHV, we expect to provide precise information concerning the biomechanics of lytic reactivation and the pathogenesis of KSHV infection.

Many previous studies have helped pave the way for the experiments detailed here, including the role of another important lytic KSHV protein, ORF59. RTA alone appears sufficient to trigger lytic reactivation, yet successful lytic DNA replication for the production of infectious KSHV virions cannot be accomplished without ORF59. ORF59, a viral protein involved in viral DNA replication, is highly expressed during lytic reactivation and during de novo primary infection (88). After forming a homodimer in the cytoplasm, ORF59 binds viral DNA polymerase and translocates to the nucleus to bind at the viral origin of lytic replication (*OriLyt*) (71, 89-91). Viral serine/threonine protein kinase (vPK), encoded by ORF36, is expressed within the first 24-48 hours of lytic

reactivation. Recently, our lab reported that the phosphorylation of ORF59 at Ser376, Ser378, and Ser379 by ORF36 is required for ORF59 to bind to replication and transcription activator (21).

Classically ORF59 is regarded as a processivity factor; however, recent studies have shown that in addition to this essential function, ORF59 associates with cellular factors to promote viral pathogenesis (92, 93). Prompted by these studies and our own data, we performed an ORF59-immunoprecipitation from KSHV infected cells, followed by protein sequencing and liquid chromatography-mass spectrometry (LC/MS) analysis to identify ORF59 interacting proteins (94). ORF59 interacting peptides, which co-precipitated with ORF59 were identified by LC/MS analysis at Mick Hitchcock Nevada Proteomics Center (University of Nevada, Reno). LC/MS results were sorted against a negative immunoprecipitation control to weed out any non-specifically interacting peptides to yield an intriguing list of novel cellular and viral binding partners.

Multiple cellular proteins were identified from the protein-protein interaction assays and the associations of some of them were confirmed through immunoprecipitation and localization assays, which are discussed here. Nucleolin (NCL) is a cellular DNA and RNA binding phosphoprotein that shuttles between the nucleus and the cytoplasm and is involved in many aspects of DNA and RNA metabolism: ribosome assembly, pre-mRNA metabolism, RNA stability, and nucleo-cytoplasmic transport (95-98). Additional cellular proteins involved with cellular DNA metabolism isolated by the ORF59 co-immunoprecipitation were the members of the minichromosome maintenance complex (MCMs). MCM proteins are replication initiation factors important for DNA replication machinery (99, 100). Lastly, a novel viral protein-protein interaction was

observed between ORF59 and KSHV ORF57. ORF57, mRNA transcript accumulation (MTA) viral early protein, is a multifunctional posttranscriptional regulator key for KSHV lytic gene expression (101). Interestingly, previous work by Majerciak et al. has shown a clear association between ORF57 protein and ORF59 RNA, but a protein-protein interaction between ORF59 and ORF57 presented a puzzling but novel avenue for investigation (102). To investigate the molecular details of ORF59 with these fascinating binding partners, we used a systematic approach to confirm protein-protein interactions, discover precise binding domains, and pinpointed the subcellular localization of these protein-protein binding occurrences.

MATERIALS AND METHODS

DNA constructs

pLVX-Flag ORF57-Flag, glutathione S-transferase ORF59-GST full-length and ORF59-GST segments, pxi-hemagglutinin (HA), ORF59-HA full-length and ORF59-HA segments were constructed by PCR amplification as previously described (21).

pA3F_MCM4-Flag, ORF59 full-length, ORF59 segments were amplified by PCR and cloned at BamHI and EcoRI restriction sites of pEGFP-C1-NLS-myc plasmid vector (60). All primers used for cloning are listed in Table 1. Flag-tagged nucleolin plasmid was a kind gift from Britt Glaunsinger (University of California, Berkeley).

Table 1. Sequences of primers used in this study (S, sense; AS, antisense).

Clones	Sense	Primer oligonucleotide sequence (5'-3')
ORF59-1A 1-198bp GFP Myc	S	CGAGCTCAAGCTTCGAATTCAATGCCTGTGGATTTT
	AS	TTATCTAGATCCGGTGGATCCAAGGGCATTCTTTAT
ORF59-1B 198-396bp GFP Myc	S	CGAGCTCAAGCTTCGAATTCAACGCCCTGGTGGGA
	AS	TTATCTAGATCCGGTGGATCCGTAGGAAATGGTGGT
ORF59-1 1-396bp GFP Myc	S	CGAGCTCAAGCTTCGAATTCAATGCCTGTGGATTTT
	AS	TTATCTAGATCCGGTGGATCCGTAGGAAATGGTGGT
ORF59-2A 396-495bp GFP Myc	S	TCT CGA GCT CAA GCT TCG AAT TCA GGG GAC AAC CTC ACC
	AS	CAG TTA TCT AGA TCC GGT GGA TCC CCT GGT GGT CCT
ORF59-2B 495-594bp GFP Myc	S	TCT CGA GCT CAA GCT TCG AAT TCA CTT CTC CTC TGT
	AS	CAG TTA TCT AGA TCC GGT GGA TCC CGT CTC GCT GAC
ORF59-2C 594-693bp GFP Myc	S	TCT CGA GCT CAA GCT TCG AAT TCA CTG TCG ATC GTG
	AS	CAG TTA TCT AGA TCC GGT GGA TCC CTT CCC CTT CAG
ORF59-2D	S	TCT CGA GCT CAA GCT TCG AAT TCA AAG TCG GTG GAT

693-792bp		
GFP Myc		
	AS	TTA TCT AGA TCC GGT GGA TCC CCA ACC CGG GAC TTT
ORF59-2 396-	S	TCT CGA GCT CAA GCT TCG AAT TCA GGG GAC AAC CTC
792bp GFP		ACC
Myc		
	AS	TTA TCT AGA TCC GGT GGA TCC CCA ACC CGG GAC TTT
ORF59-3A	S	CGAGCTCAAGCTTCGAATTCATTTACCCCCGGGCTG
793-991bp		
GFP Myc		
	AS	TTATCTAGATCCGGTGGATCCAGACTCCAATTCCGG
ORF59-3B	S	CGAGCTCAAGCTTCGAATTCACCGGATTCTCCCCCT
991-1188bp		
GFP Myc		
	AS	TTATCTAGATCCGGTGGATCCAATCAGGGGGTAAA*
ORF59-3 793-	S	CGAGCTCAAGCTTCGAATTCATTTACCCCCGGGCTG
1188 GFP		
Myc		
	AS	TTATCTAGATCCGGTGGATCCAATCAGGGGGTAAA
MCM4-Flag	S	TACCGAGCTCGGATCCGCCATGTCGTCCCCGGCGTCGACCCCG
	AS	GATATCTGCAGAATTCCGAGCAAGCGCACGGTCTTCCCAGTC

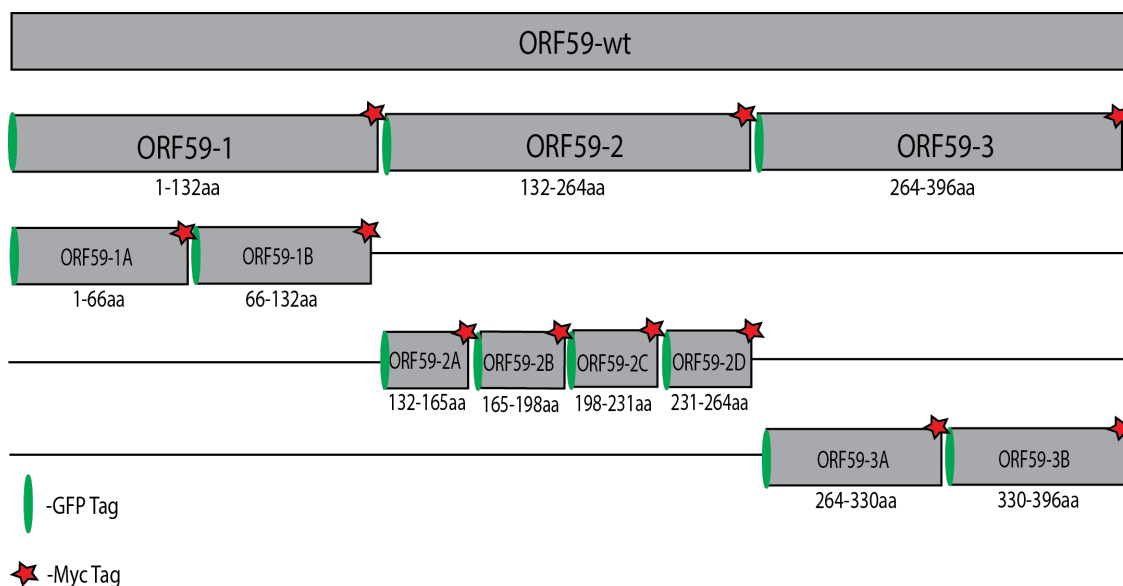


Figure 1: Schematic illustrating the ORF59GFP and Myc epitope tagged segments used for binding assays.

Cell Culture and transfection

HEK293T cells were purchased from ATCC and maintained in Dulbecco's modified Eagle's medium (DMEM) (Fisher Scientific Co., Pittsburgh, PA) supplemented with 10% bovine growth serum (BGS, HyClone, Logan, UT), 2 mM L-glutamine, 25 U/mL penicillin, and 25 μ g/mL streptomycin. The TRExBCBL-1/RTA cell line was cultured in RPMI 1640 medium supplemented with 10% Tet-free FBS, 2mM L-glutamine, 25U/mL penicillin, 25 μ g/mL streptomycin and 20 ug/ml hygromycin B. TREX-BCBL-1/RTA is a KSHV-positive B cell line with doxycycline-inducible lytic cycle switch RTA gene. The iSLKBAC16-wt and iSLK.219 cell lines were a generous gift from Dr. Jae U. Jung (Keck School of medicine, USC). These cell lines were grown in DMEM supplemented with 10% FBS, 2mM L-glutamine, 25U/mL penicillin, 25 μ g/mL streptomycin, along with 1 ug/ml puromycin, 250 ug/ml G418 and 1.2 mg/ml hygromycin B. All cell lines were grown at 37°C in a humidified chamber supplemented with 5% CO₂. HEK293T

cells were transfected with 1 mg/ml of polyethyleneimine (PEI) at a ratio of 1 ug plasmid DNA: 3ul PEI. To induce lytic expression, TrexBCBL-1/RTA cells were treated with 1 ug/ml of doxycycline (Dox), whereas both the iSLKBAC16-wt and iSLK.219 cells were treated with 1 ug/ml of doxycycline (Dox) and 1mM sodium butyrate, for the indicated times.

Immunoprecipitation and Immunoblotting

Cells were transfected, harvested, washed with ice-cold phosphate-buffered saline (PBS), and lysed in 0.8 ml ice-cold radioimmunoprecipitation assay (RIPA) buffer (1% Nonidet P-40 [NP-40], 10mM Tris [pH 7.5], 2mM EDTA, 150mM NaCl) supplemented with protease inhibitors (1mM phenylmethylsulfonyl fluoride, 1µg/ml aprotinin, 1µg/ml pepstatin, 1µg/ml leupeptin, and 1µg/ml sodium fluoride (Sigma-Aldrich)). Cells were centrifuged at 5,000 x g (8 min and 4°C) to remove cell debris, and lysates were precleared for 1 h by rotation at 4°C with 25 µl of protein A-protein G-conjugated Sepharose beads. After approximately 5% of the lysate was saved for use as an input control, the target protein was captured by rotating the remainder of the lysate with 1 µg of appropriate antibody overnight at 4°C. Immune complexes were captured with 50 µl of protein A-protein G-conjugated Sepharose beads by rotation at 4°C for 2 hrs. The beads were pelleted and washed three times with 500 µl RIPA buffer. Input lysates and immunoprecipitated complexes were boiled for 6 to 8 min in Laemmli buffer, resolved by SDS-PAGE, transferred to nitrocellulose membrane, and blocked in 5% milk as per the manufacturer's recommendation (Bio-Rad Laboratories). The associated antibodies were used to probe the nitrocellulose membrane, incubated with 1% milk containing the

appropriate infrared dye-tagged secondary antibody, and scanned using an Odyssey imager (LICOR Inc., Lincoln, NE).

The following antibodies were used to probe the immunoblots: mouse anti-Flag (M2; Sigma-Aldrich, St. Louis, MO), rabbit anti-HA (6908; Sigma-Aldrich Corp., St. Louis, MO), mouse anti-GST (A00014; GenScript Corp.), mouse anti-Myc (Sigma-Aldrich Corp., St. Louis, MO), mouse anti-Nucleolin 4E2 (ab13541; Abcam), rabbit anti-KSHV ORF57 (SAB1305667; Sigma-Aldrich Corp., St. Louis, MO).

Purification of GST fusion proteins

Constructs for ORF59-GST fusion proteins were expressed in *Escherichia coli* strain BL21 (DE3) cells. Briefly, bacterial culture for each construct was incubated in an orbital shaker and the cells were induced with 1mM (final concentration) isopropyl- β -D-thiogalactopyranoside (IPTG) for 4 h at 37°C. The cells were centrifuged and the bacterial pellet was washed once with 5 ml STE buffer (100mM NaCl, 10mM Tris, 1mM EDTA, pH 7.5) and resuspended in 5 ml NETN buffer (0.5% NP-40, 100mM NaCl, 20mM Tris, 1mM EDTA, pH 8.0) supplemented with protease inhibitors (Sigma-Aldrich). Cells were then lysed using STE buffer containing 75 μ l of 1M dithiothreitol (DTT) and 900 μ l of 10% Sarkosyl solution, incubated on ice for 15 min and sonicated using a microtip sonicator for 4 min at 30W with 20-sec on/off pulses (the lysate should appear clear/opaque and not cloudy). The cell debris was removed by centrifugation at 13,000 x g for 10 min at 4°C. The lysate was treated with 1.5 ml of 10% Triton X-100 (in STE buffer) and 200 μ l of glutathione-Sepharose beads for affinity purification. After incubation overnight at 4°C with rotation, the samples were centrifuged 600 x g for 2 min

at 4°C to collect the purified proteins bound to glutathione beads. Beads were washed 5 times with NETN buffer supplemented with protease inhibitors and the GST protein expression levels and purity were determined using SDS-PAGE and western blot assay.

Immunofluorescence microscopy

For fluorescence microscopy, iSLKBAC16-wt were grown on coverslips and lytic cycle was induced with 1 ug/ml of doxycycline (Dox) and 1mM sodium butyrate. At 48 h post-transfection, cells were incubated with 30 uM EdU (5-ethynyl-2'-deoxyuridine) to label the newly synthesized DNA for 30 min, and fixed with 4% (v/v) formaldehyde for 10 min at room temperature. After PBS washes, the cells were permeabilized with 0.2% Triton X-100 for 18 min at room temperature. The cells were subsequently washed three times with 1X PBS. Click reaction was performed to conjugate biotin to the EdU-labeled DNA. Cells were incubated in a click reaction buffer containing cell buffer additive, 2mM CuSO₄ and 5 uM biotin-azide (Life Technologies, Inc.) for 30 min. DMSO was added instead of biotin-azide to the negative control samples. Cells were washed three times with 1X PBS and blocked in 0.4% fish skin gelatin (FSG, Sigma-Aldrich) and 0.05% Triton X-100 for 45 min at room temperature. Cells were washed three times with 1X PBS and incubated with primary antibody (0.2% FSG, 0.05% Triton X-100, 0.5 µg antibody) for 1 h at room temperature. Cells were washed three times with 1X PBS and treated with secondary antibody (0.2% FSG, 0.05% Triton X-100, 1:1000 dilution of stock antibody). The nuclei was stained with 1 ug/mL TO-PRO-3 for 1 min and the cells/coverslips were washed three times with 1X PBS, mounted onto glass slides and dried at 37°C. Alexa Fluor -conjugated antibodies: AF488, AF594, and AF647 were used

for the detection of ORF59, Nucleolin and EdU, respectively, as indicated in the immune localization panels. Images were obtained using a laser scanning confocal microscope (Carl Zeiss, Inc.) and processed with ZEN imaging software (Carl Zeiss, Inc.) to assign the appropriate color.

RESULTS

As many independent roles have been assigned to KSHV ORF59, we first needed to generate a series of truncation mutants of ORF59 to methodically determine the specific amino acid domains of ORF59, which serves as a contact domain with these newly identified binding partners of ORF59. A series of ORF59 domains were cloned into overexpression plasmids containing GFP and the Myc epitope tag (Fig. 1). By expressing these recombinant ORF59 truncations within the cells along with the binding partner of interest, we were able to pinpoint the distinct regions of ORF59 facilitating the interaction.

ORF59 and NCL associate endogenously and *in vitro*:

Nucleolin is the most abundant non-ribosomal protein in nucleolus and is conserved in vertebrates with protein analogs in plants and yeast (96, 103, 104). Thus, to confirm the specific association of Nucleolin (NCL) and ORF59, we performed co-immunoprecipitation assays as well as *in vitro* binding assays. iSLKBAC16WT cells were induced for lytic replication for 48 hours using doxycycline. Cell lysate was incubated for co-immunoprecipitation assay with control rabbit anti-IgG, rabbit anti-ORF57, and rabbit anti-ORF59 overnight at 4°C. The samples were resolved using SDS-PAGE followed by

western blotting. Five percent of total lysate for inputs was acquired (Fig. 2A, lane 1). Using mouse anti-NCL antibody, bands were detected indicating an association of NCL with ORF57 (Fig. 2A, lane 3) and ORF59 (Fig. 2A, lane 4). The control IgG antibody was unable to co-precipitate the proteins, suggesting a specific interaction (Fig. 2A, lane 2).

For *in vitro* binding assay, HEK293T cells were transfected with NCL-Flag and lysate was incubated with ORF59-GST full length or individual segments overnight at 4°C. SDS-PAGE and western blotting were used to resolve the samples. ORF59-GST full length and segments were purified according to GST protein purification protocol. Input levels were normalized across samples, the amount represented in Fig. 2B, lane 1. ORF59-GST (Fig. 2B, lane 3) and ORF59-1-GST (1-132aa) (Fig. 2B, lane 4) were found to bind NCL-Flag. In contrast, control GST was incubated with lysate and no binding was observed (Fig. 2B, lane 2). Nucleolin was not detected in lanes 5 and 6, suggesting that ORF59-2 and ORF59-3 (132-396aa) do not serve as the binding domain for Nucleolin. (Fig. 2B, lanes 5 and 6).

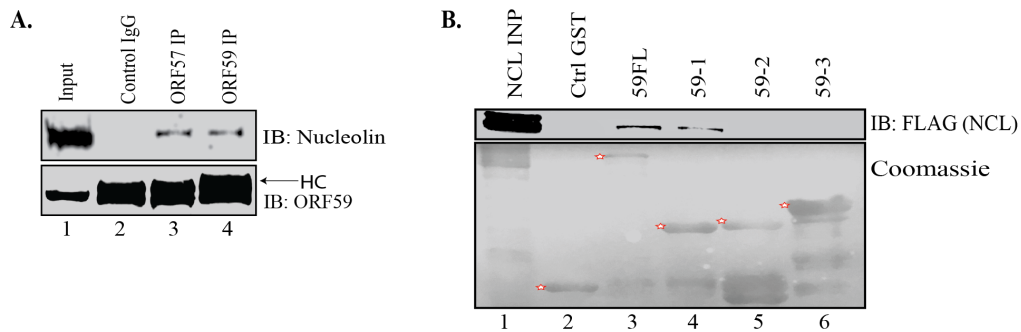


Figure 2: ORF59 associates with Nucleolin. (A) iSLKBac16WT cells were induced for lytic replication for 48 hours, crosslinked using formaldehyde, lysed, treated with RNase H, and immunoprecipitation with anti-ORF57 and anti-ORF59 antibody was performed. Five percent of input was taken from total lysate (lane 1). Anti-ORF57 coprecipitated NCL (lane 3) and anti-ORF59 coprecipitated NCL (lane 4). Control IgG antibody was unable to coprecipitate NCL (lane 2). (B) HEK293T cells were transfected with NCL-Flag and lysate was incubated with ORF59-GST-fused constructs for *in-vitro* binding assays. Five percent of total lysate was collected for input column (lane 1). ORF59 binds NCL where recombinant ORF59-GST (lane 3) and ORF59-1-GST (lane 4) coprecipitated with NCL-Flag. ORF59-2-GST (lane 5) and ORF59-3-GST (lane 6) were unable to coprecipitate with NCL-Flag. Control GST did not coprecipitate NCL-Flag (lane 2).

ORF59 associates with NCL in the nuclei of lytically reactivating cells:

Given NCL's role in the nuclear export of mRNA to the cytoplasm, and ORF59's role in shuttling viral DNA polymerase to the nucleus, we were eager to determine the subcellular localization of ORF59 and NCL. To this end, KSHV positive endothelial cells, iSLKs harboring the KSHV bacterial artificial chromosome BAC16WT (referred to as iSLKBAC16WT cells from here onwards) were grown on cover slips and induced for lytic replication for 48 hours using doxycycline and sodium butyrate. The corresponding uninduced (latent) controls were cultivated on coverslips in Tet-free media.

Immunofluorescence assay was performed as described in materials and methods, using primary antibodies for mouse anti-NCL and rabbit anti-ORF59 and secondary antibodies,

AF594 and AF647, respectively. Nucleolin was consistently detected in the nucleoli, lining the replication compartments, in both uninduced and 48 hour induced samples (Fig. 3, panels I and V). NCL expression was located in the nucleus, which was demarcated by TO-PRO-3 nuclear staining (not shown). In addition to lining the replication compartments in induced cells, NCL was perceived as many dispersed speckles distributed within the nucleus and cytoplasm (Fig. 3, panel V). Punctate expression of ORF59, a marker of KSHV lytic replication, was observed in the nucleus and cytoplasm of lytically reactivated cells (Fig. 3, panel VI) and was not seen in uninduced cells, as expected (Fig. 3, panel II). Size, number, and shape of replication compartments were variable from cell to cell. Upon lytic induction for 48 hours, ORF59 and NCL were found to colocalize in the nuclei (Fig. 3, panel VII). Differential interference contrast (DIC) microscope images were obtained to depict transparent cell morphology (Fig. 3, panel IV and VIII). Multiple optical fields were analyzed and the levels of colocalization between ORF59 and NCL were determined. Colocalization coefficients ($c = \text{pixels}_{\text{Channel 59}} / \text{pixels}_{\text{Channel NCL}}$) were calculated and averaged across optical fields. The average colocalization coefficient between ORF59 and NCL was 81.1% based on analysis of at least 10 independent cells. In summary, these images may suggest a cooperative role for ORF59 and NCL in nuclei of reactivating cells.

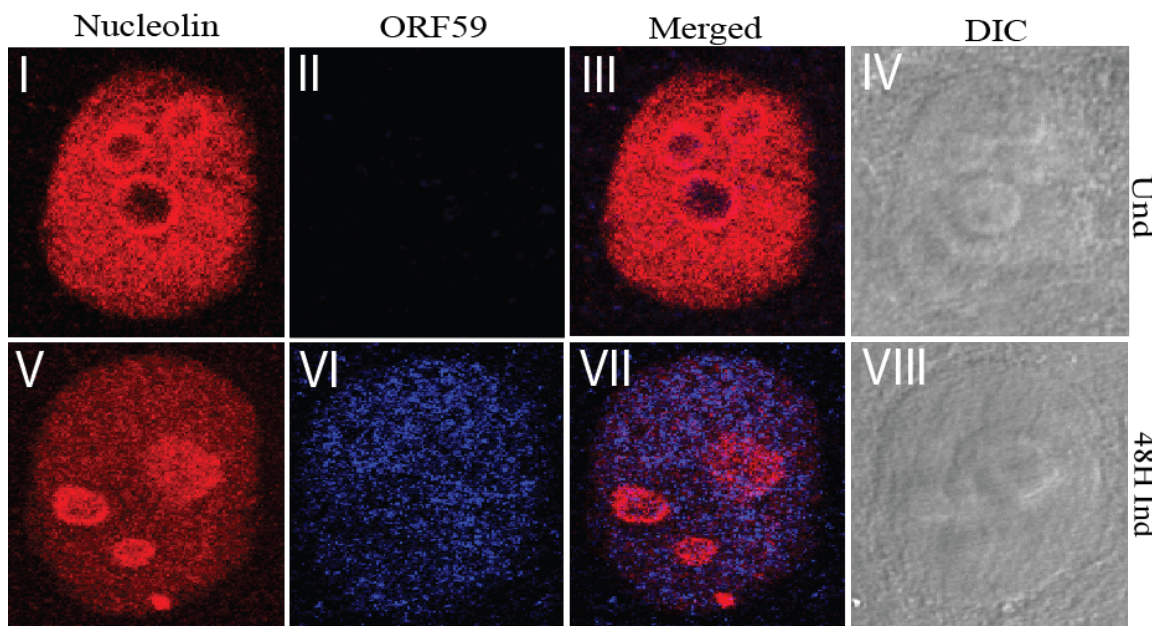


Figure 3: ORF59 and NCL colocalize during lytic reactivation. iSLKBAC16WT were grown on coverslips, induced for lytic reactivation for 48 hours, fixed, blocked, labeled with primary antibodies for anti-NCL and anti-ORF59, and secondary antibodies for AF594 (shown in red) and AF647 (shown in blue). The subcellular localization of ORF59 and NCL was visualized by immunofluorescence microscopy. NCL and ORF59 proteins were not observed to colocalize in uninduced cells (panel III). Colocalization of NCL and ORF59 proteins was observed in 48 hour induced cells (panel VII). DIC images were used for confirmation of cell viability (panel IV and VIII).

ORF59 and ORF57 associate endogenously:

After confirming the interaction with KSHV ORF59 and cellular RNA-processing factor NCL, we sought to confirm the novel interaction between ORF59 and the virally-encoded mRNA processing protein, ORF57, which had been indicated by our LC/MS screen. ORF57 (mRNA transcript accumulation factor) is conserved amongst all human herpesviruses. This viral protein functions to promote efficient expression of viral genes (including ORF59) through a variety of regulatory functions in RNA stability, RNA splicing, and protein translation activation. To determine if these two viral proteins bind

during lytic reactivation, we used KSHV positive iSLK.219 cells to test for an endogenous association. For these purposes, iSLK.219 cells were induced for lytic reactivation for 24 and 48 hours using doxycycline and sodium butyrate. Lysate was incubated with rabbit anti-ORF59 antibody at 4°C for overnight rotation. SDS-PAGE and western blotting were used to resolve the samples. Inputs for 24 and 48 hour induced samples were obtained for comparison (Fig. 4 lanes 1 and 2). Rabbit anti-ORF57 antibody was used to detect bands in both 24 and 48 hour induced samples, suggesting an ORF57 association with ORF59 at both time points (Fig. 4 lanes 3 and 4). Interestingly, endogenous binding between ORF59 and ORF57 appeared more robust in 48 hour induced samples (lane 4).

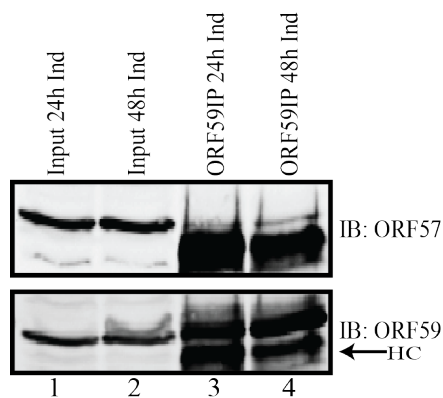


Figure 4: ORF59 and ORF57 associate endogenously. iSLK.219 cells were induced for lytic replication for 24 or 48 hours, lysed, and immunoprecipitation was done with anti-ORF59 antibody. Inputs representing five percent of total lysate were taken (lanes 1 and 2). ORF59 specific antibody immunoprecipitated ORF59, and coprecipitated ORF57 at 24 and 48 hours (lanes 3 and 4). Control IgG was used to ensure that these interactions are specific (data not shown).

ORF59 and ORF57 interact directly via specific domain:

Next, it was important to determine if the endogenous interaction demonstrated between ORF59 and ORF57 proteins, as shown in Fig. 4, was in fact a direct protein-protein interaction or is perhaps facilitated by other lytic factors present during KSHV reactivation. To this end, we examined the binding between these proteins in the absence of KSHV infection. First, HEK293T cells were co-transfected with epitope tagged constructs for ORF59-HA and ORF57-Flag. Input control (Fig. 5A, lane 1) lane confirmed the expression of the recombinant epitope-tagged viral proteins. Anti-flag ORF57 immunoprecipitation showed a clear, specific pull-down of ORF57 (compare ORF57 bands in Fig. 5A lane 3, with IgG control, lane 2). Furthermore, full-length ORF59 HA (ORF59-FL in Fig. 5A), co-precipitated with ORF57-Flag, but not with control IgG antibody.

In addition, we assessed binding between ORF59 and ORF57 *in vitro*. GST-tagged control protein, or ORF59 were purified as described in materials and methods. ORF57-Flag was expressed in HEK293T cells transfected with recombinant ORF57-Flag plasmid and the successful overexpression of flag-tagged ORF57 was indicated in the input lane (Fig. 5B, lane 1). The ORF57-Flag cell lysate was combined with equal amounts of either control-GST or ORF59-GST and incubated overnight at 4°C. Samples were washed and proteins were resolved using SDS-PAGE and western blot methods. ORF59-GST was clearly able to pull-down ORF57-Flag while in contrast no ORF57-Flag could be detected co-precipitating with control-GST. These results show a robust interaction between ORF59 and ORF57 proteins, independent of other KSHV proteins.

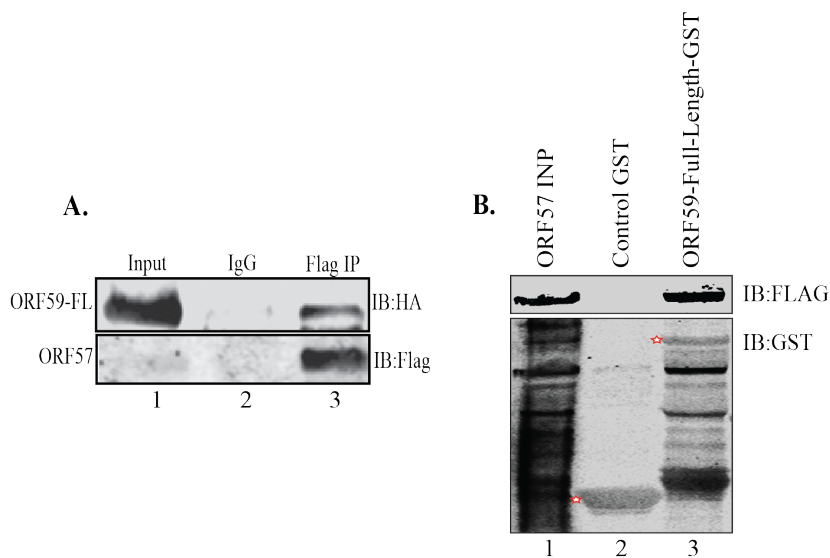


Figure 5: ORF59 and ORF57 proteins associate directly. (A) HEK293T cells were cotransfected with ORF59-HA and ORF57-Flag, lysed, and five percent input was taken from whole lysate (lane 1). Anti-Flag antibody was used to immunoprecipitate ORF57-Flag, which coprecipitated ORF59-HA (lane 3). Control IgG antibody was unable to coprecipitate (lane 2). (B) HEK293T cells were transfected with ORF57-Flag and lysate was incubated with ORF59-GST-fused constructs for *in-vitro* binding assays. Five percent lysate was collected for input column (lane 1). ORF59-GST was able to coprecipitate with ORF57-Flag (lane 3). Control GST was not able to coprecipitate with ORF57-Flag (lane 2).

Following the determination of ORF59's interaction with ORF57, we wanted to identify the region(s) of ORF59 responsible for interacting with ORF57. Using an *in vitro* approach, control-GST, or full-length ORF59 and truncated sections of GST fused ORF59 segments were purified, and incubated with equal amounts of ORF57-Flag expressing HEK293T cell lysates (ample ORF57-Flag expression is demonstrated in Fig. 6A, lane 1). We expected ORF59-full length to precipitate ORF57-Flag (Fig. 6A, lane 3), but perplexingly each GST truncation of ORF59 also co-precipitated ORF57-Flag from cell lysate. The interaction between ORF59 and ORF57 appeared to be strongest between

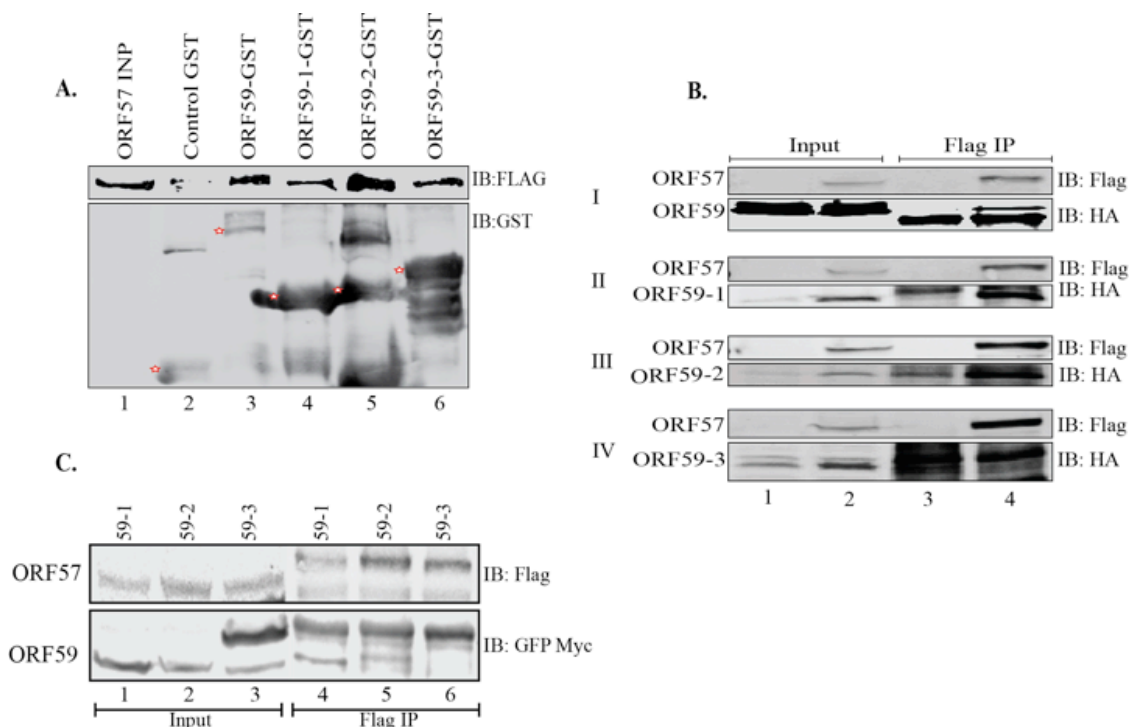


Figure 6: ORF59 1-264aa associates with ORF57: (A) HEK293T cells were transfected with ORF57-Flag, lysed, and incubated with ORF59-GST full-length and segments for *in-vitro* studies. Five percent of lysate was kept for input sample (lane 1). ORF59-1-GST and ORF59-3-GST were able to coprecipitate with ORF57-Flag (lanes 4 and 6). ORF59-GST-full-length and ORF59-2-GST illustrated more robust binding with ORF57-Flag (lanes 3 and 5). Control GST did not coprecipitate ORF57-Flag (lane 2). (B) HEK293T cells were cotransfected with ORF59-HA full-length and segments and ORF57-Flag, lysed, and five percent input was extracted (lanes 1 and 2). Immunoprecipitation was performed with anti-Flag antibody. ORF57 was able to coprecipitate ORF59 full-length, ORF59-1 (rows I and II, lane 4). ORF57 was not able to coprecipitate ORF59-3 (row IV, lane 4). (C) HEK293T cells were co-transfected with ORF57-FLAG and ORF59-GFP-myc segments, lysed, and anti-Flag immunoprecipitation was performed. Five percent of entire lysate were extracted for inputs (lanes 1-3). ORF57 was able to coprecipitate ORF59-1 and ORF59-2 (lanes 4 and 5). ORF59-3 was unable to coprecipitate (lane 6).

full-length ORF59, and ORF59 132-264aa. Despite the seemingly broad interaction domains between ORF59 and ORF57 indicated by this *in vitro* experiment (Fig. 6A lanes 3-6), the control-GST did not coprecipitate ORF57, suggesting the interaction between ORF59 and ORF57 is nevertheless specific to these proteins, and not mediated by non-specific experimental conditions (Fig. 6A, lane 2).

In an effort to narrow down a specific ORF59 binding domain, HEK293T cells were co-transfected with ORF57-Flag or Pa3F and ORF59-HA full-length and ORF59-HA segments. Cells were lysed for co-IP assay and incubated with mouse anti-Flag overnight at 4°C. Mouse anti-Flag and rabbit anti-HA were used to detect ORF57-Flag, ORF59-HA full-length, and ORF59-HA segments respectively. Input controls (Fig. 6B, lanes 1 and 2) show expression levels of ORF59 truncation mutants and ORF59 full length. ORF57 was able to robustly coprecipitate ORF59-HA full-length (Fig. 6B, row I, lane 4), and ORF59-1-HA segment (1-132aa) (Fig. 6B, row II, lane 4). ORF57 didn't appear to co-precipitate ORF59-2-HA segment or ORF59-3-HA segment (132-396aa) (Fig. 6B, rows III and IV, lane 4). Empty Flag vector, Pa3F, was used as a control with ORF59-HA full-length and segments during co-transfection to ensure binding specificity (Fig. 6B, lanes 1 and 3).

Since ORF57-Flag demonstrated binding with ORF59 full length, in addition to 1-264aa segments of ORF59, we wanted to combine the ORF57-Flag immunoprecipitation into a single gel to test comparative binding strength between ORF57 with ORF59 segments. To this end, HEK293T cells with plasmids expressing epitope tagged versions of ORF57-Flag and ORF59-GFP-myc segments, were lysed for co-IP assay using mouse anti-Flag overnight at 4°C. Lysates were taken as input controls, which showed comparable levels of each ORF59 truncation (Fig. 6C, lanes 1-3). ORF57 co-precipitated ORF59-1-GFP-myc (1-132aa) (Fig. 6C, lane 4) and ORF59-2-GFP-myc (132-264aa) (Fig. 6C, lane 5) with seemingly equal intensity but did not co-precipitate ORF59-3-GFP-myc (264-396aa). This suggests that regions of ORF59 (1-264aa) are essential for the

protein-protein interaction with ORF57 and that the C-terminal domain of ORF59 truncation is not required for this interaction.

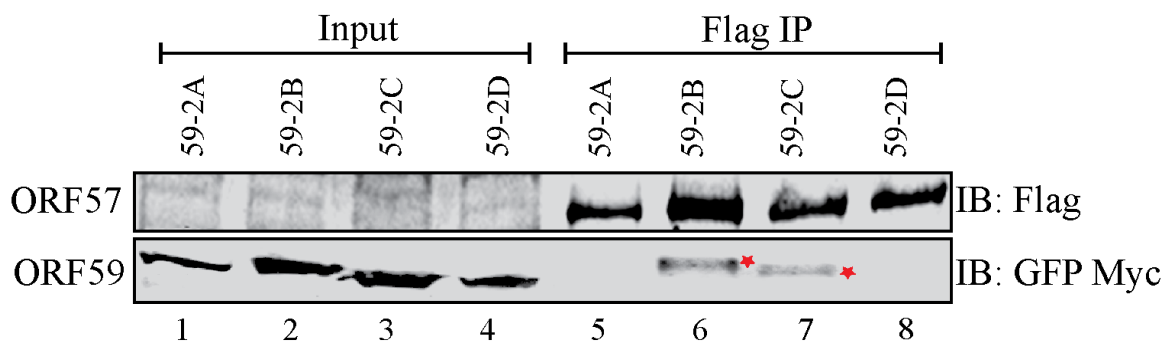


Figure 7: ORF59 segment 2 subsegments associate with ORF57 in an overexpression system. HEK293T cells were co-transfected with ORF57-Flag and ORF59-2-GFP-myc segments. Cells were lysed for coimmunoprecipitation assay and incubated with anti-Flag antibody. Five percent of whole lysates were taken as inputs (lanes 1-4). ORF57 was found to coprecipitate ORF59-2B (lane 6) and ORF59-2C (lane 7) favorably. ORF57 did not coprecipitate ORF59-2A (lane 5) and ORF59-2C (lane 8).

Previous studies characterizing functional binding domains of ORF59 have similarly determined this same region of ORF59 (1-264aa), as a protein-protein interaction domain (21, 94) and thus it was fairly unsurprising that ORF57 associates with this domain as well. Our goal was to determine whether the unique ORF59 domain binding to ORF57 could be isolated by using smaller ORF59 truncated segments to discern a smaller interaction domain between ORF59 and ORF57. Sub-sections of ORF59 132-264aa (refer to Fig. 1), representing individual 33aa domains of ORF59 were co-transfected with ORF57-Flag. The cells were lysed, precleared, and incubated overnight at 4°C for co-IP assay. Input fractions show similar expression levels from lane to lane of ORF57-flag and each ORF59-2 segment (Fig. 7, lanes 1-4). ORF57-Flag was immunoprecipitated, which was capable of distinctly co-immunoprecipitating ORF59-2B-GFP-myc (165-198aa) (Fig. 7, lane 6) and ORF59-2C-GFP-myc (198-231aa) (Fig. 7,

lane 7). In contrast, ORF59-2A-GFP-myc (132-165aa) (Fig. 7, lane 5) and ORF59-2D-GFP-myc (231-264aa) (Fig. 7, lane 8) were unable to establish explicit binding. This indicated the specific binding domain of ORF59 (165-231aa) to be imperative for ORF57 and ORF59 protein-protein interaction.

ORF59 interacts with cellular DNA replication licensing factor MCM4:

The MCM proteins, MCMs 2-7, specifically, form a hexameric complex that is loaded at cellular origins of DNA replication during G1 phase of the cell cycle. This leads to a recruitment of DNA polymerase for the replication of DNA. As licensing factors, these proteins are responsible for ensuring that only a single round of DNA replication takes place during that cell cycle, so it's unsurprising that MCMs are documented to be aberrantly overexpressed in proliferating cells and cells licensed for DNA replication, meaning they are specific biomarkers for cancer detection (99, 105). Furthermore, other herpesviruses have been shown to de-regulate MCM proteins and interfere with host DNA synthesis and cell cycle progression, but as of yet no functional studies have investigated the role of MCMs during lytic KSHV reactivation. Due to the multifunctional roles of ORF59 during lytic reactivation, we were eager to confirm an association between ORF59 and the MCM proteins. Six individual MCM proteins associate to form a hexameric complex with a critical role in cellular DNA replication licensing; however, clues from a previous study done in EBV where researchers discovered that MCM4 was abnormally phosphorylated by virally-encoded kinase during lytic reactivation led us to first investigate a direct association between MCM4 and ORF59.

This association was first tested in an overexpression system by cotransfecting HEK293T cells with MCM4-Flag or Pa3F and ORF59-GFP-myc full-length and segments. Cells were lysed for co-IP assay and incubated with mouse anti-Flag overnight at 4°C. Mouse anti-Flag and mouse anti-Myc were used. Input lanes confirm expression of ORF59 segments although levels of MCM4-Flag in the lysate were only faintly detected (Fig. 8, lanes 1 and 2). MCM4 was found to associate with ORF59-1-GFP-myc (1-132aa) (Fig. 8, row I, lane 4) and ORF59-2-GFP-myc (132-264aa) (Fig. 8, row II, lane 4) but did not exhibit binding with ORF59-3-GFP-myc (264-396aa) (Fig. 8, row III, lane 4). Flag vector controls also co-transfected with each ORF59 segment, but did not exhibit any affinity for the ORF59 proteins, demonstrating a specific interaction between MCM4-flag and ORF59 1-264aa (Fig. 8, rows I, II lane 3).

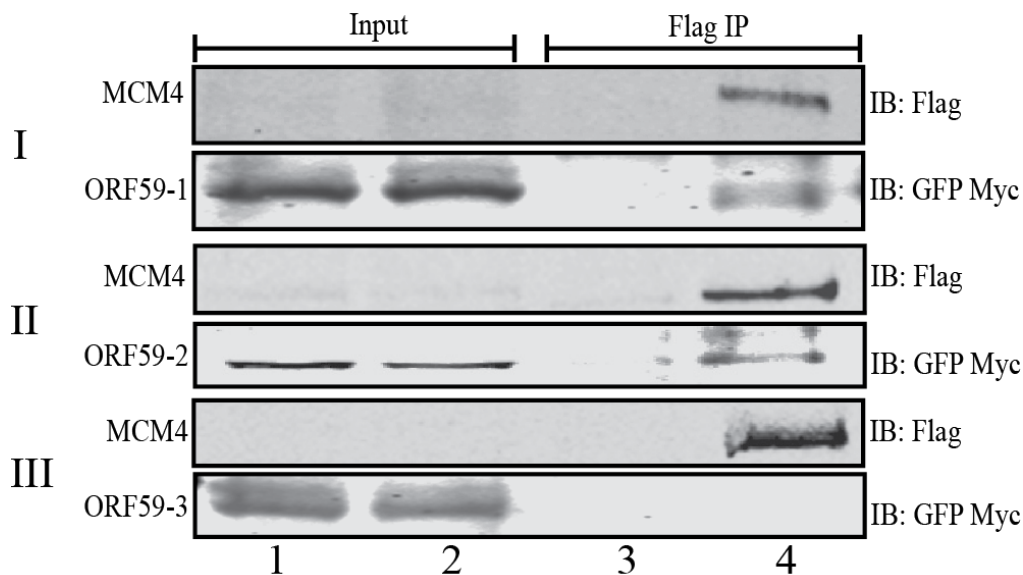


Figure 8: ORF59 truncations domains associate with MCM4 in an overexpression system. HEK293T cells were cotransfected with MCM4-Flag and ORF59-GFP-myc segments, lysed, and incubated with anti-Flag antibody for coimmunoprecipitation assay. Five percent lysate was taken for inputs (lanes 1 and 2). MCM4 coprecipitated ORF59-1-GFP-myc (row I, lane 4) and ORF59-2-GFP-myc (row II, lane 4). MCM4 was not able to coprecipitate ORF59-3-GFP-myc (row III, lane 4). Empty flag vector (Pa3F) was used as a control for specific binding (lanes 1 and 3).

To narrow down a more definitive binding region of ORF59 with MCM4, subsections of ORF59 (detailed in Fig. 1), were co-transfected in HEK293T cells with recombinant plasmids expressing MCM4-Flag and ORF59-2-GFP-myc and truncations 59-2A, 59-2B, 59-2C, and 59-2D cloned in GFP-Myc vector. Cell lysates were precleared and incubated for co-IP assay overnight at 4°C. Inputs controls were taken for each sample (Fig. 9, lanes 1-5) and only slight variability is observed between ORF59 truncation expression levels. MCM4-flag expression is only faintly detected in lysate, but anti-Flag antibody demonstrated a robust immunoprecipitation of MCM4 (Fig. 9, lanes 6-10).

MCM4-Flag was immunoprecipitated using anti-Flag antibody and was able to co-precipitate ORF59-2B-GFP-myc (165-198aa) (Fig. 9, lane 7), ORF59-2C-GFP-myc (198-231aa) (Fig. 9, lane 8), and ORF59-2-GFP-myc (132-264aa) (Fig. 9, lane 10). MCM4 did appear to coprecipitate ORF59-2A-GFP-myc (132-165aa) (Fig. 9, lane 6) or ORF59-2D-GFP-myc (231-264aa) (Fig. 9, lane 9). Flag-vector alone was unable to co-precipitate any of the ORF59 truncations (data not shown). In this manner, we determined the minimal ORF59 binding domain for interaction with MCM4 to be ORF59 165-231aa.

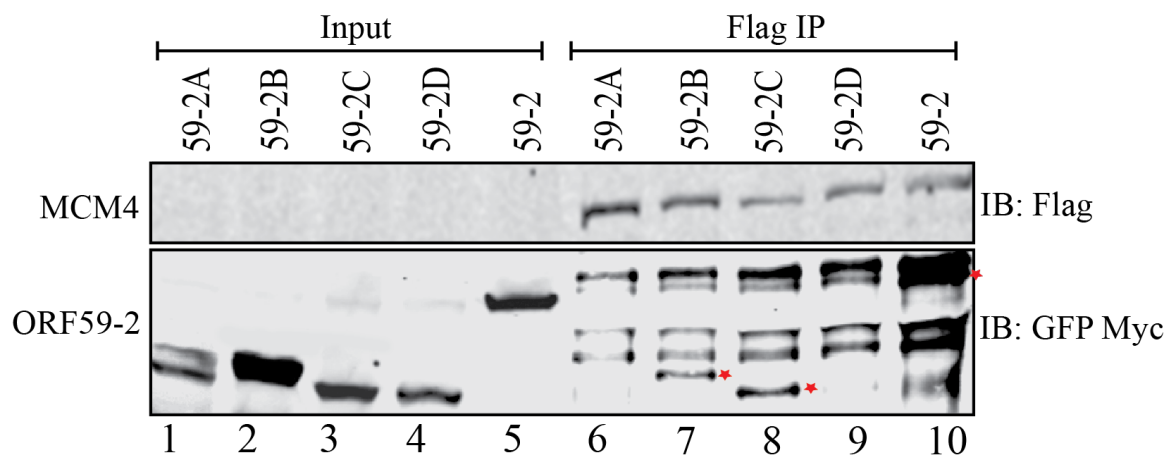


Figure 9: ORF59 Segment 2 subsegments associate with MCM4 in an overexpression system. HEK293T cells were cotransfected with MCM4-Flag and ORF59-2-GFP-myc and segments, lysed, and incubated with anti-Flag for coimmunoprecipitation assay. Five percent total lysate was taken for each input sample (lanes 1-5). MCM4 was able to coprecipitate ORF59-2B (lane 7), ORF59-2C (lane 8), and ORF59-2 (lane 10). MCM4 was not able to coprecipitate 59-2A (lane 6) or 59-2D (lane 9).

Given that ORF59 is an essential component of KSHV DNA replication, and the MCM complexes are involved in cellular DNA replication licensing, we were interested in evaluating the subcellular localization of these factors during lytic reactivation. TRexBCBL-1/RTA cells were grown in T-25 flasks and induced for lytic replication for 24 hours using doxycycline and sodium butyrate. Cells were incubated with EdU to label actively replicating KSHV DNA (Fig. 10, panel VIII) or DMSO for negative control (Fig. 10, panel III). Cells were fixed onto coverslips and Click-iT chemistry protocol was used to identify actively replicating DNA. Afterward, primary antibody for rabbit anti-ORF59 (Fig. 10, panels I and VI) and mouse anti-MCM4 (Fig. 10, panels II and VII) were applied to the coverslips for overnight. The next day, secondary antibodies, AF488, AF594, and AF647 were applied for 45 minutes and the coverslips were mounted. As expected, during lytic reactivation ORF59 displayed a punctate

nuclear expression pattern (Fig. 10, panels I, VI). MCM4 was also dispersed within cell nuclei, and at certain loci was found to co-localize with ORF59 (Fig. 10, panel IV, note cyan-colored areas). The DMSO channel (Fig. 10, panel III) of the infected cell shown in panels I-V did not display any signal indicating the Click-iT chemistry used is demarcating actively replicating DNA (Fig. 10, panel VIII) in the cell displayed in panels VI-X, and was not simply binding to cellular compartments non-specifically. Shown in the merge panel (Fig. 10, panel IX) there are points of yellow pigment, which represent the co-localization of ORF59 with actively replicating KSHV DNA. Notably, in this same panel hardly any instances of MCM4 co-localizing with actively replicating DNA, cellular or otherwise are observed (magenta pixels in Fig. 10, panel IX), although once again MCM4 does appear to co-localize with ORF59 at various loci (cyan pixels, Fig. 10, panel IX). Differential interference contrast (DIC) microscope imaging was

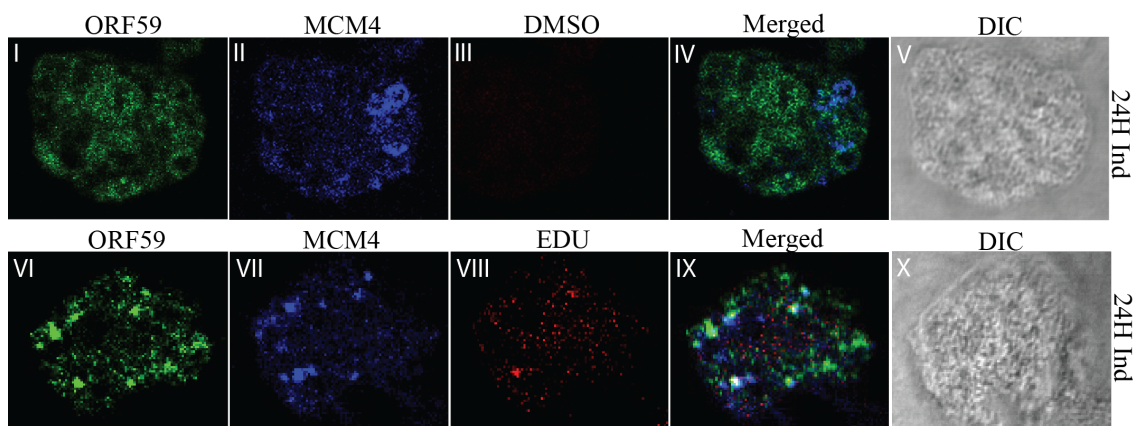


Figure 10: ORF59 and MCM4 colocalize during lytic reactivation. TrexBCBL-1/RTA cells were induced for lytic replication for 24 hours, incubated with EdU to label replicating KSHV DNA, fixed, blocked, and Click-iT chemistry was performed. Then samples were labeled with primary antibodies for anti-ORF59 and anti-MCM4, and secondary antibodies for AF488, AF594, and AF647. A laser scanning confocal microscope was used to visualize the subcellular localization of the proteins and capture images. MCM4 and ORF59 proteins were observed to colocalize at some foci in 24 hour induced cells (panel IX). Another set of 24 hour induced cells were incubated with DMSO as a control instead of EDU for Click-iT chemistry (panel III). DIC images were taken to depict cell morphology (panels V and X).

used to assess cell health (Fig. 10, panel V and X). Mean values were determined across optical fields. Based on at least 10 different cells, we determined the average colocalization coefficient of 69.3% between ORF59 and MCM4. This suggests a complicated arrangement of the nuclear replication compartments where ORF59's colocalization with MCM4 could be disrupting the association of MCM4 with actively replicating cellular DNA.

DISCUSSION:

During lytic reactivation, KSHV orchestrates the ordered synthesis of numerous viral products that are responsible for viral DNA synthesis, virion assembly, and egress of infectious viral particles. Viral DNA processivity factor, ORF59, is an early lytic protein expressed during de novo primary infection as well as during lytic reactivation and is absolutely essential for efficient viral DNA replication (21, 71, 88, 91, 106, 107). In other herpesviruses, the homologs of ORF59 are necessary for DNA replication. Homologs of ORF59 include: Herpes Simplex-1 (HSV-1) UL42, Epstein-Barr Virus (EBV) BMRF1, Herpesvirus Saimiri (HVS) ORF59, Human Cytomegalovirus (HCMV) ICP36/UL44, Human Herpesvirus-6 (HHV-6) p41, Varicella-Zoster Virus (VZV) gene 16 protein, and Human Herpesvirus-7 (HHV-7) U27 (9, 88, 90, 108). Our LC/MS analysis of ORF59 binding peptides revealed several intriguing interaction partners. Out of which, viral protein ORF57, and cellular proteins Nucleolin (NCL) and MCM4, were pursued for the purposes of this study.

KSHV ORF57 (mRNA transcript accumulation factor) has displayed involvement in posttranscriptional processing of viral transcripts including: increasing viral RNA

stability, RNA splicing, and protein translation (64, 101, 109-122). In fact, ORF57 enhances the stability of ORF59 mRNA by preventing hyperpolyadenylation of ORF59 mRNA by RBM15, resulting in higher levels of ORF59 protein expression (123-126). PAN lncRNA is another viral RNA protected from degradation in the nucleus by ORF57 binding to PABPC1 on Mta-responsive element (MRE hairpin), likely contributing to the very high copy number of PAN RNA in lytic cells (estimated at 5×10^5 copies/cell) (119, 127, 128). Given the seemingly unrelated roles of ORF57 in viral mRNA processing, and ORF59 in DNA processivity, it was puzzling but intriguing when we identified ORF57 as a binding partner of ORF59. We were able to confirm this association endogenously at 24h and 48h time points during lytic reactivation. Arguably, during lytic reactivation an association between ORF59 may be mediated through other factors, with one likely candidate being PAN lncRNA, which independent studies have shown to associate with ORF57, and ORF59 (110, 129). While further experiments are necessary to rule out the assistance of PAN RNA in the binding of ORF59 and ORF57, we nevertheless show that these proteins do not require any additional viral factors to facilitate their association as binding between these proteins could be detected in an over-expression and *in-vitro* systems and takes place along the 165-231aa region of ORF59. The direct nature of this interaction suggests that ORF59 could be involved in a previously unsuspected role of assisting ORF57 with viral mRNA processing.

This hypothesis actually begins to hold water in light of our data confirming the interaction between ORF59 and cellular NCL. NCL's role in eukaryotic cells involves ribosome biogenesis and maturation, and NCL directly interacts with pre-rRNA transcripts to promote cell growth (130). Interestingly, many groups have reported NCL's

involvement during several different viral infections including EBV, HCMV, and even previous work on KSHV (131-136). During KSHV lytic replication, NCL is reported to be directed from the nucleolar subcompartment of the nucleus into the cytoplasm where it binds to the IL-6 3' UTR and protects transcripts from degradation by viral nuclease SOX (ORF37) (136). Also during lytic reactivation, we show that KSHV ORF59 and NCL bind and colocalize in the nuclei of the infected cells, suggesting NCL's involvement with multiple viral proteins during lytic infection. This was not surprising, considering human cytomegalovirus (HCMV) UL44 protein (homolog of KSHV ORF59) associated with and co-localized with NCL in HCMV-infected cells and was suggested to be necessary for maintaining the architecture of replication compartments (135, 137).

Interestingly, Boyne and Whitehouse characterized a relationship between NCL and ORF57 in KSHV-infected cells (115). Although ORF57 promotes KSHV intronless RNA expression for many viral genes, it does not possess the capabilities for direct export of viral RNAs (117). Boyne and Whitehouse show that together with Nucleolin, ORF57 mediates the nucleolar shuttling of intronless viral mRNAs (115). In this context, our results suggest the association of ORF59 and ORF57 to mechanistically facilitate efficient translation of viral transcripts during lytic replication and supports our hypothesis that a relationship involving ORF59, NCL, and ORF57 is important for efficient lytic reactivation (109, 138, 139).

In reality, this mechanism may be an excellent target for therapeutic development of KSHV treatments based on previous work done in EBV to target NCL. Epstein-Barr Virus (EBV) nuclear antigen 1 (EBNA1) is a genome maintenance protein that helps EBV to persist as an episome during latency and functions to promote transcription of

viral genes. Nucleolin is an important co-factor to facilitate the EBNA1 binding interaction with oriP (133). Very recently Lista and colleagues found that NCL directly interacts with the G-quadruplexes formed in the glycine-alanine repeats of EBNA1 mRNA to suppress EBNA1 expression as a means of immune evasion during EBV infection; furthermore, this interaction could be targeted by treatment with G4 ligand, PhenDC3 to stimulate EBNA1 expression and antigen presentation (140). While further studies are needed to gain a more complete understanding of the significance of NCL and its association with viral proteins, ORF59 and ORF57, our work nonetheless supports a novel avenue for the discovery of future therapeutics.

Clues from work done on other herpesviruses EBV and HCMV also provide insight as to the significance of the interaction we characterized between ORF59 and cellular DNA replication licensing factor, MCM4. Our work showed that ORF59 interacts with MCM4 in an overexpression system, which demonstrated that these proteins are capable of interacting even in the absence of KSHV infection. Since ORF59 and MCM4 both have DNA-binding capabilities, we were curious to determine if ORF59 may be playing a role in deregulating cellular MCMs from cellular replication origins. Under normal conditions, DNA replication origins licensing is dependent upon the MCM complex proteins and numerous cofactors in the replication complex, and pre-replication complex ORCs, and Cdc6, Cdt1, Cdc45, and DDK. MCMs are assembled in the nuclear matrix as a part of the pre-replication complex (pre-RC) along with poly (ADP-ribose) polymerase 1 (PARP1), origin recognition complex (ORC), and cell division cycle (Cdc6) proteins (141, 142). Every G1 phase, origins of replication are licensed (reactivated) at origins by the assembly of pre-replication complex (pre-RC), in which

MCM complex is loaded onto chromatin (143). We speculate that the normal function of MCM proteins are de-regulated during KSHV lytic reactivation, likely through MCM4's interaction with ORF59. This notion is also supported by our IFA results, which showed startlingly little overlap between MCM4 and actively replicating cellular DNA in lytically reactivating cells. As a matter of fact, Wiebusch et al. determined that HCMV inhibits assembly of pre-replication complex (pre-RC) and prevents MCM loading onto chromatin, stopping cellular DNA replication (143). One possible mechanism for carrying out this sabotage of cellular DNA replication KSHV could employ has been implicated by research performed in EBV. In EBV, MCM4 is phosphorylated by EBV protein kinase (EBV-PK) encoded by BGLF4 during lytic replication, resulting in loss of helicase activity and cell cycle arrest (144). Considering KSHV ORF59's direct interaction with (and subsequent phosphorylation by) the viral kinase ORF36, we speculate that these KSHV lytic proteins may work in concert to possibly aberrantly phosphorylate MCM4 and disrupt binding of the hexameric MCM complex from cellular origins.

The objective of these experiments was to collect biomechanical information concerning the interactions between ORF59 and these binding partners. The development of effective therapeutics for patients suffering from KSHV infection faces many challenges. For example, drugs which target a particular viral protein ultimately prompt the virus to mutate and develop resistance. On the other hand, compounds that target cellular proteins often have rather high toxicity meaning very bad side effects for the patient. Our unique approach to carefully understand minute interactions between

viral and host proteins therefore offers a novel strategy for the identification of therapeutic targets, which may be exploited for regulating KSHV mediated pathogenesis.

FUTURE DIRECTIONS:

These data provide exciting preliminary prospects for further investigation. We are planning to visualize the colocalization of ORF59 and ORF57 in KSHV-positive cells, as it will be important for determining the functional applications of this interaction to know whether the interaction takes place in the nucleus or cytoplasm. In addition, we will conduct an RNA stability assay in ORF59 and ORF57 depleted cells to determine if ORF59 may have some synergistic effects on ORF57's mRNA processing duties.

Also, since NCL's subcellular location is regulated by its phosphorylational state, we intend to evaluate a potential association between KSHV viral kinase, ORF36 and NCL, which we suspect is mediated by ORF59. NCL is usually phosphorylated by many kinases: casein kinase II (CK2), Cdc2 (Cdk1), stress-activated protein kinase (SAPK) p38, and protein kinase C (PKC) (145-148). In cells, we will perform an *in vitro* kinase assay and resolve samples using the Phos-tag reagent to test whether ORF36 is actively phosphorylating NCL. This same assay will also be applied to test for aberrant phosphorylation of MCM proteins as a means of KSHV upsetting cellular DNA replication and cell cycle progression.

In summary, our results suggest a common model utilized by herpesviruses, which frequently hijack cellular machinery to promote their own life cycles where viral factors, ORF59 and ORF57 associate with cellular RNA processing machinery (NCL) to ensure an efficient production of infectious virions following lytic reactivation. This

research will provide a better understanding of host-virus interactions during KSHV lytic replication and is anticipated to contribute to identification of therapeutic avenues for blocking KSHV pathogenesis.

REFERENCES

1. Soulier J, Grollet L, Oksenhendler E, Cacoub P, Cazals-Hatem D, Babinet P, d'Agay MF, Clauvel JP, Raphael M, Degos L, et al. Kaposi's sarcoma-associated herpesvirus-like DNA sequences in multicentric Castleman's disease. *Blood*. 1995;86(4):1276-80. PubMed PMID: 7632932.
2. Bhutani M, Polizzotto MN, Uldrick TS, Yarchoan R. Kaposi sarcoma-associated herpesvirus-associated malignancies: epidemiology, pathogenesis, and advances in treatment. *Semin Oncol*. 2015;42(2):223-46. doi: 10.1053/j.seminoncol.2014.12.027. PubMed PMID: 25843728.
3. Grundhoff A, Sullivan CS, Ganem D. A combined computational and microarray-based approach identifies novel microRNAs encoded by human gamma-herpesviruses. *RNA*. 2006;12(5):733-50. Epub 2006/03/17. doi: 10.1261/rna.2326106. PubMed PMID: 16540699; PMCID: PMC1440911.
4. Studahl M, Hagberg L, Rekadbar E, Bergstrom T. Herpesvirus DNA detection in cerebral spinal fluid: differences in clinical presentation between alpha-, beta-, and gamma-herpesviruses. *Scand J Infect Dis*. 2000;32(3):237-48. Epub 2000/07/06. PubMed PMID: 10879592.
5. Banerjee S, Uppal T, Strahan R, Dabral P, Verma SC. The Modulation of Apoptotic Pathways by Gammaherpesviruses. *Front Microbiol*. 2016;7:585. Epub 2016/05/21. doi: 10.3389/fmicb.2016.00585. PubMed PMID: 27199919; PMCID: PMC4847483.
6. Dourmishev LA, Dourmishev AL, Palmeri D, Schwartz RA, Lukac DM. Molecular genetics of Kaposi's sarcoma-associated herpesvirus (human herpesvirus-8) epidemiology and pathogenesis. *Microbiol Mol Biol Rev*. 2003;67(2):175-212, table of contents. PubMed PMID: 12794189; PMCID: 156467.
7. Ganem D. KSHV and the pathogenesis of Kaposi sarcoma: listening to human biology and medicine. *J Clin Invest*. 2010;120(4):939-49. doi: 10.1172/JCI40567. PubMed PMID: 20364091; PMCID: 2847423.
8. Arias C, Weisburd B, Stern-Ginossar N, Mercier A, Madrid AS, Bellare P, Holdorf M, Weissman JS, Ganem D. KSHV 2.0: a comprehensive annotation of the Kaposi's sarcoma-associated herpesvirus genome using next-generation sequencing reveals novel genomic and functional features. *PLoS Pathog*. 2014;10(1):e1003847. doi: 10.1371/journal.ppat.1003847. PubMed PMID: 24453964; PMCID: 3894221.
9. Russo JJ, Bohenzky RA, Chien MC, Chen J, Yan M, Maddalena D, Parry JP, Peruzzi D, Edelman IS, Chang Y, Moore PS. Nucleotide sequence of the Kaposi sarcoma-associated herpesvirus (HHV8). *Proc Natl Acad Sci U S A*. 1996;93(25):14862-7. PubMed PMID: 8962146; PMCID: PMC26227.
10. Choi J, Means RE, Damania B, Jung JU. Molecular piracy of Kaposi's sarcoma associated herpesvirus. *Cytokine Growth Factor Rev*. 2001;12(2-3):245-57. PubMed PMID: 11325605.

11. Verma SC, Robertson ES. Molecular biology and pathogenesis of Kaposi sarcoma-associated herpesvirus. *FEMS Microbiol Lett.* 2003;222(2):155-63. PubMed PMID: 12770701.
12. O'Connor CM, Kedes DH. Rhesus monkey rhadinovirus: a model for the study of KSHV. *Curr Top Microbiol Immunol.* 2007;312:43-69. Epub 2006/11/09. PubMed PMID: 17089793.
13. Klein G. Herpesviruses and oncogenesis. *Proc Natl Acad Sci U S A.* 1972;69(4):1056-64. Epub 1972/04/01. PubMed PMID: 4337235; PMCID: PMC426626.
14. Perkins EM, Anacker D, Davis A, Sankar V, Ambinder RF, Desai P. Small capsid protein pORF65 is essential for assembly of Kaposi's sarcoma-associated herpesvirus capsids. *J Virol.* 2008;82(14):7201-11. doi: 10.1128/JVI.00423-08. PubMed PMID: 18463150; PMCID: PMC2446949.
15. Trus BL, Heymann JB, Nealon K, Cheng N, Newcomb WW, Brown JC, Kedes DH, Steven AC. Capsid structure of Kaposi's sarcoma-associated herpesvirus, a gammaherpesvirus, compared to those of an alphaherpesvirus, herpes simplex virus type 1, and a betaherpesvirus, cytomegalovirus. *J Virol.* 2001;75(6):2879-90. doi: 10.1128/JVI.75.6.2879-2890.2001. PubMed PMID: 11222713; PMCID: PMC115914.
16. Wang X, Zhu N, Li W, Zhu F, Wang Y, Yuan Y. Mono-ubiquitylated ORF45 Mediates Association of KSHV Particles with Internal Lipid Rafts for Viral Assembly and Egress. *PLoS Pathog.* 2015;11(12):e1005332. Epub 2015/12/10. doi: 10.1371/journal.ppat.1005332. PubMed PMID: 26650119; PMCID: PMC4674120.
17. Akula SM, Pramod NP, Wang FZ, Chandran B. Human herpesvirus 8 envelope-associated glycoprotein B interacts with heparan sulfate-like moieties. *Virology.* 2001;284(2):235-49. doi: 10.1006/viro.2001.0921. PubMed PMID: 11384223.
18. Chakraborty S, Veetil MV, Chandran B. Kaposi's Sarcoma Associated Herpesvirus Entry into Target Cells. *Front Microbiol.* 2012;3:6. doi: 10.3389/fmicb.2012.00006. PubMed PMID: 22319516; PMCID: PMC3262161.
19. Bechtel JT, Liang Y, Hvidding J, Ganem D. Host range of Kaposi's sarcoma-associated herpesvirus in cultured cells. *J Virol.* 2003;77(11):6474-81. PubMed PMID: 12743304; PMCID: PMC155009.
20. Chang Y, Cesarman E, Pessin MS, Lee F, Culpepper J, Knowles DM, Moore PS. Identification of herpesvirus-like DNA sequences in AIDS-associated Kaposi's sarcoma. *Science.* 1994;266(5192):1865-9. PubMed PMID: 7997879.
21. McDowell ME, Purushothaman P, Rossetto CC, Pari GS, Verma SC. Phosphorylation of Kaposi's sarcoma-associated herpesvirus processivity factor ORF59 by a viral kinase modulates its ability to associate with RTA and oriLyt. *J Virol.* 2013;87(14):8038-52. doi: 10.1128/JVI.03460-12. PubMed PMID: 23678174; PMCID: 3700218.
22. Polizzotto MN, Uldrick TS, Wyvill KM, Aleman K, Marshall V, Wang V, Whitby D, Pittaluga S, Jaffe ES, Millo C, Tosato G, Little RF, Steinberg SM, Sereti I, Yarchoan R. Clinical Features and Outcomes of Patients With Symptomatic Kaposi Sarcoma Herpesvirus (KSHV)-associated Inflammation: Prospective Characterization of KSHV

- Inflammatory Cytokine Syndrome (KICS). *Clin Infect Dis*. 2016;62(6):730-8. doi: 10.1093/cid/civ996. PubMed PMID: 26658701; PMCID: PMC4772848.
23. Cohen A, Wolf DG, Guttman-Yassky E, Sarid R. Kaposi's sarcoma-associated herpesvirus: clinical, diagnostic, and epidemiological aspects. *Crit Rev Clin Lab Sci*. 2005;42(2):101-53. doi: 10.1080/10408360590913524. PubMed PMID: 15941082.
 24. Cheung TW. AIDS-related cancer in the era of highly active antiretroviral therapy (HAART): a model of the interplay of the immune system, virus, and cancer. "On the offensive--the Trojan Horse is being destroyed"--Part A: Kaposi's sarcoma. *Cancer Invest*. 2004;22(5):774-86. PubMed PMID: 15581058.
 25. Gbabe OF, Okwundu CI, Dedicoat M, Freeman EE. Treatment of severe or progressive Kaposi's sarcoma in HIV-infected adults. *Cochrane Database Syst Rev*. 2014(9):CD003256. doi: 10.1002/14651858.CD003256.pub2. PubMed PMID: 25313415.
 26. Ploegh HL. Viral strategies of immune evasion. *Science*. 1998;280(5361):248-53. PubMed PMID: 9535648.
 27. Yewdell JW, Hill AB. Viral interference with antigen presentation. *Nat Immunol*. 2002;3(11):1019-25. doi: 10.1038/ni1102-1019. PubMed PMID: 12407410.
 28. Andrei G, Snoeck R. Kaposi's sarcoma-associated herpesvirus: the role of lytic replication in targeted therapy. *Curr Opin Infect Dis*. 2015;28(6):611-24. doi: 10.1097/QCO.0000000000000213. PubMed PMID: 26524334.
 29. Coen N, Duraffour S, Snoeck R, Andrei G. KSHV targeted therapy: an update on inhibitors of viral lytic replication. *Viruses*. 2014;6(11):4731-59. doi: 10.3390/v6114731. PubMed PMID: 25421895; PMCID: 4246246.
 30. Giffin L, Damania B. KSHV: pathways to tumorigenesis and persistent infection. *Adv Virus Res*. 2014;88:111-59. doi: 10.1016/B978-0-12-800098-4.00002-7. PubMed PMID: 24373311; PMCID: 4104069.
 31. Sellar RS, Peggs KS. Management of multidrug-resistant viruses in the immunocompromised host. *Br J Haematol*. 2012;156(5):559-72. doi: 10.1111/j.1365-2141.2011.08988.x. PubMed PMID: 22188225.
 32. Upadhyayula S, Michaels MG. Ganciclovir, Foscarnet, and Cidofovir: Antiviral Drugs Not Just for Cytomegalovirus. *J Pediatric Infect Dis Soc*. 2013;2(3):286-90. doi: 10.1093/jpids/pit048. PubMed PMID: 26619485.
 33. Delice S, Gokahmetoglu S, Kaynar L, Karakukcu M. [Investigation of ganciclovir resistance in CMV UL54 and UL97 gene regions in immunocompromised patients receiving ganciclovir treatment]. *Mikrobiyol Bul*. 2015;49(3):393-402. PubMed PMID: 26313280.
 34. Martin JN. The epidemiology of KSHV and its association with malignant disease. In: Arvin A, Campadelli-Fiume G, Mocarski E, Moore PS, Roizman B, Whitley R, Yamanishi K, editors. *Human Herpesviruses: Biology, Therapy, and Immunoprophylaxis*. Cambridge2007.
 35. Labo N, Miley W, Benson CA, Campbell TB, Whitby D. Epidemiology of Kaposi's sarcoma-associated herpesvirus in HIV-1-infected US persons in the era of

- combination antiretroviral therapy. *AIDS*. 2015;29(10):1217-25. doi: 10.1097/QAD.0000000000000682. PubMed PMID: 26035321.
36. La Ferla L, Pinzone MR, Nunnari G, Martellotta F, Lleshi A, Tirelli U, De Paoli P, Berretta M, Cacopardo B. Kaposi's sarcoma in HIV-positive patients: the state of art in the HAART-era. *Eur Rev Med Pharmacol Sci*. 2013;17(17):2354-65. PubMed PMID: 24065230.
37. Epelbaum O, Go R, Patel G, Braman S. Pulmonary Kaposi's Sarcoma and Its Complications in the HAART Era: A Contemporary Case-Based Review. *Lung*. 2016;194(1):163-9. doi: 10.1007/s00408-015-9830-7. PubMed PMID: 26826066.
38. Paparizos VA, Kyriakis KP, Kourkounti S, Leuow K, Daskalakis E, Katsambas A. The Influence of a HAART regimen on the expression of HIV-associated Kaposi sarcoma. *J Acquir Immune Defic Syndr*. 2008;49(1):111. doi: 10.1097/QAI.0b013e31816d9d2b. PubMed PMID: 18725809.
39. McLaughlin-Drubin ME, Munger K. Viruses associated with human cancer. *Biochim Biophys Acta*. 2008;1782(3):127-50. Epub 2008/01/19. doi: 10.1016/j.bbadis.2007.12.005. PubMed PMID: 18201576; PMCID: PMC2267909.
40. Vieira J, O'Hearn P, Kimball L, Chandran B, Corey L. Activation of Kaposi's sarcoma-associated herpesvirus (human herpesvirus 8) lytic replication by human cytomegalovirus. *J Virol*. 2001;75(3):1378-86. Epub 2001/01/11. doi: 10.1128/JVI.75.3.1378-1386.2001. PubMed PMID: 11152511; PMCID: PMC114044.
41. Zhou F, Xue M, Qin D, Zhu X, Wang C, Zhu J, Hao T, Cheng L, Chen X, Bai Z, Feng N, Gao SJ, Lu C. HIV-1 Tat promotes Kaposi's sarcoma-associated herpesvirus (KSHV) vIL-6-induced angiogenesis and tumorigenesis by regulating PI3K/PTEN/AKT/GSK-3beta signaling pathway. *PLoS One*. 2013;8(1):e53145. Epub 2013/01/10. doi: 10.1371/journal.pone.0053145. PubMed PMID: 23301033; PMCID: PMC3534639.
42. Zhu X, Guo Y, Yao S, Yan Q, Xue M, Hao T, Zhou F, Zhu J, Qin D, Lu C. Synergy between Kaposi's sarcoma-associated herpesvirus (KSHV) vIL-6 and HIV-1 Nef protein in promotion of angiogenesis and oncogenesis: role of the AKT signaling pathway. *Oncogene*. 2014;33(15):1986-96. Epub 2013/04/23. doi: 10.1038/onc.2013.136. PubMed PMID: 23604117.
43. Roupelieva M, Griffiths SJ, Kremmer E, Meisterernst M, Viejo-Borbolla A, Schulz T, Haas J. Kaposi's sarcoma-associated herpesvirus Lana-1 is a major activator of the serum response element and mitogen-activated protein kinase pathways via interactions with the Mediator complex. *J Gen Virol*. 2010;91(Pt 5):1138-49. Epub 2010/01/22. doi: 10.1099/vir.0.017715-0. PubMed PMID: 20089804.
44. Tang Q, Qin D, Lv Z, Zhu X, Ma X, Yan Q, Zeng Y, Guo Y, Feng N, Lu C. Herpes simplex virus type 2 triggers reactivation of Kaposi's sarcoma-associated herpesvirus from latency and collaborates with HIV-1 Tat. *PLoS One*. 2012;7(2):e31652. Epub 2012/02/22. doi: 10.1371/journal.pone.0031652. PubMed PMID: 22347501; PMCID: PMC3276581.
45. Lu C, Zeng Y, Huang Z, Huang L, Qian C, Tang G, Qin D. Human herpesvirus 6 activates lytic cycle replication of Kaposi's sarcoma-associated herpesvirus. *Am J*

- Pathol. 2005;166(1):173-83. Epub 2005/01/06. doi: 10.1016/S0002-9440(10)62242-0. PubMed PMID: 15632010; PMCID: PMC1602294.
46. Blauvelt A. Skin diseases associated with human herpesvirus 6, 7, and 8 infection. *J Investig Dermatol Symp Proc.* 2001;6(3):197-202. Epub 2002/04/02. doi: 10.1046/j.0022-202x.2001.00040.x. PubMed PMID: 11924827.
47. Rady PL, Yen A, Martin RW, 3rd, Nedelcu I, Hughes TK, Tyring SK. Herpesvirus-like DNA sequences in classic Kaposi's sarcomas. *J Med Virol.* 1995;47(2):179-83. Epub 1995/10/01. PubMed PMID: 8830123.
48. Mercader M, Taddeo B, Panella JR, Chandran B, Nickoloff BJ, Foreman KE. Induction of HHV-8 lytic cycle replication by inflammatory cytokines produced by HIV-1-infected T cells. *Am J Pathol.* 2000;156(6):1961-71. Epub 2000/06/15. doi: 10.1016/S0002-9440(10)65069-9. PubMed PMID: 10854219; PMCID: PMC1850066.
49. Ye F, Lei X, Gao SJ. Mechanisms of Kaposi's Sarcoma-Associated Herpesvirus Latency and Reactivation. *Adv Virol.* 2011;2011. Epub 2011/06/01. doi: 10.1155/2011/193860. PubMed PMID: 21625290; PMCID: PMC3103228.
50. Osmond DH, Buchbinder S, Cheng A, Graves A, Vittinghoff E, Cossen CK, Forghani B, Martin JN. Prevalence of Kaposi sarcoma-associated herpesvirus infection in homosexual men at beginning of and during the HIV epidemic. *JAMA.* 2002;287(2):221-5. Epub 2002/01/12. PubMed PMID: 11779265.
51. Hayward GS. Human herpesvirus 8 latent-state gene expression and apoptosis in Kaposi's sarcoma lesions. *J Natl Cancer Inst.* 1999;91(20):1705-7. PubMed PMID: 10528012.
52. Fu B, Yang R, Xia F, Li B, Ouyang X, Gao SJ, Wang L. Gender differences in Kaposi's sarcoma-associated herpesvirus infection in a population with schistosomiasis in rural China. *Jpn J Infect Dis.* 2012;65(4):350-3. Epub 2012/07/21. PubMed PMID: 22814163; PMCID: PMC3513380.
53. Wang X, Zou Z, Deng Z, Liang D, Zhou X, Sun R, Lan K. Male hormones activate EphA2 to facilitate Kaposi's sarcoma-associated herpesvirus infection: Implications for gender disparity in Kaposi's sarcoma. *PLoS Pathog.* 2017;13(9):e1006580. Epub 2017/09/29. doi: 10.1371/journal.ppat.1006580. PubMed PMID: 28957431; PMCID: PMC5619820.
54. Lebbe C, Porcher R, Marcelin AG, Agbalika F, Dussaix E, Samuel D, Varnous S, Euvrard S, Bigorie A, Creusvaux H, Legendre C, Frances C, Skin, Organ Transplantation Group of the French Society of D. Human herpesvirus 8 (HHV8) transmission and related morbidity in organ recipients. *Am J Transplant.* 2013;13(1):207-13. doi: 10.1111/j.1600-6143.2012.04290.x. PubMed PMID: 23057808.
55. Kaleeba JA, Berger EA. Broad target cell selectivity of Kaposi's sarcoma-associated herpesvirus glycoprotein-mediated cell fusion and virion entry. *Virology.* 2006;354(1):7-14. doi: 10.1016/j.virol.2006.06.009. PubMed PMID: 16889811.
56. Ballestas ME, Kaye KM. The latency-associated nuclear antigen, a multifunctional protein central to Kaposi's sarcoma-associated herpesvirus latency.

- Future Microbiol. 2011;6(12):1399-413. doi: 10.2217/fmb.11.137. PubMed PMID: 22122438; PMCID: PMC3857968.
57. Knipe DM, Lieberman PM, Jung JU, McBride AA, Morris KV, Ott M, Margolis D, Nieto A, Nevels M, Parks RJ, Kristie TM. Snapshots: chromatin control of viral infection. *Virology*. 2013;435(1):141-56. Epub 2012/12/12. doi: 10.1016/j.virol.2012.09.023. PubMed PMID: 23217624; PMCID: PMC3531885.
58. Verma SC, Choudhuri T, Kaul R, Robertson ES. Latency-associated nuclear antigen (LANA) of Kaposi's sarcoma-associated herpesvirus interacts with origin recognition complexes at the LANA binding sequence within the terminal repeats. *J Virol*. 2006;80(5):2243-56. doi: 10.1128/JVI.80.5.2243-2256.2006. PubMed PMID: 16474132; PMCID: 1395374.
59. Verma SC, Cai Q, Kreider E, Lu J, Robertson ES. Comprehensive analysis of LANA interacting proteins essential for viral genome tethering and persistence. *PLoS One*. 2013;8(9):e74662. doi: 10.1371/journal.pone.0074662. PubMed PMID: 24040311; PMCID: PMC3770571.
60. Xiao B, Verma SC, Cai Q, Kaul R, Lu J, Saha A, Robertson ES. Bub1 and CENP-F can contribute to Kaposi's sarcoma-associated herpesvirus genome persistence by targeting LANA to kinetochores. *J Virol*. 2010;84(19):9718-32. doi: 10.1128/JVI.00713-10. PubMed PMID: 20660191; PMCID: PMC2937805.
61. Verma SC, Robertson ES. ORF73 of herpesvirus Saimiri strain C488 tethers the viral genome to metaphase chromosomes and binds to cis-acting DNA sequences in the terminal repeats. *J Virol*. 2003;77(23):12494-506. PubMed PMID: 14610173; PMCID: 262571.
62. Antman K, Chang Y. Kaposi's sarcoma. *N Engl J Med*. 2000;342(14):1027-38. doi: 10.1056/NEJM200004063421407. PubMed PMID: 10749966.
63. Sun R, Lin SF, Staskus K, Gradoville L, Grogan E, Haase A, Miller G. Kinetics of Kaposi's sarcoma-associated herpesvirus gene expression. *J Virol*. 1999;73(3):2232-42. PubMed PMID: 9971806; PMCID: 104468.
64. Malik P, Blackburn DJ, Cheng MF, Hayward GS, Clements JB. Functional cooperation between the Kaposi's sarcoma-associated herpesvirus ORF57 and ORF50 regulatory proteins. *J Gen Virol*. 2004;85(Pt 8):2155-66. doi: 10.1099/vir.0.79784-0. PubMed PMID: 15269354.
65. Song MJ, Deng H, Sun R. Comparative study of regulation of RTA-responsive genes in Kaposi's sarcoma-associated herpesvirus/human herpesvirus 8. *J Virol*. 2003;77(17):9451-62. PubMed PMID: 12915560; PMCID: PMC187374.
66. Seaman WT, Quinlivan EB. Lytic switch protein (ORF50) response element in the Kaposi's sarcoma-associated herpesvirus K8 promoter is located within but does not require a palindromic structure. *Virology*. 2003;310(1):72-84. Epub 2003/06/06. PubMed PMID: 12788632.
67. Song MJ, Brown HJ, Wu TT, Sun R. Transcription activation of polyadenylated nuclear rna by rta in human herpesvirus 8/Kaposi's sarcoma-associated herpesvirus. *J Virol*. 2001;75(7):3129-40. doi: 10.1128/JVI.75.7.3129-3140.2001. PubMed PMID: 11238840; PMCID: PMC114107.

68. Bu W, Palmeri D, Krishnan R, Marin R, Aris VM, Soteropoulos P, Lukac DM. Identification of direct transcriptional targets of the Kaposi's sarcoma-associated herpesvirus Rta lytic switch protein by conditional nuclear localization. *J Virol.* 2008;82(21):10709-23. doi: 10.1128/JVI.01012-08. PubMed PMID: 18715905; PMCID: PMC2573185.
69. Deng H, Song MJ, Chu JT, Sun R. Transcriptional regulation of the interleukin-6 gene of human herpesvirus 8 (Kaposi's sarcoma-associated herpesvirus). *J Virol.* 2002;76(16):8252-64. Epub 2002/07/23. PubMed PMID: 12134031; PMCID: PMC155161.
70. Byun H, Gwack Y, Hwang S, Choe J. Kaposi's sarcoma-associated herpesvirus open reading frame (ORF) 50 transactivates K8 and ORF57 promoters via heterogeneous response elements. *Mol Cells.* 2002;14(2):185-91. PubMed PMID: 12442889.
71. Rossetto CC, Susilarini NK, Pari GS. Interaction of Kaposi's sarcoma-associated herpesvirus ORF59 with oriLyt is dependent on binding with K-Rta. *J Virol.* 2011;85(8):3833-41. doi: 10.1128/JVI.02361-10. PubMed PMID: 21289111; PMCID: 3126130.
72. Ueda K, Ishikawa K, Nishimura K, Sakakibara S, Do E, Yamanishi K. Kaposi's sarcoma-associated herpesvirus (human herpesvirus 8) replication and transcription factor activates the K9 (vIRF) gene through two distinct cis elements by a non-DNA-binding mechanism. *J Virol.* 2002;76(23):12044-54. PubMed PMID: 12414946; PMCID: PMC136869.
73. Bowser BS, Morris S, Song MJ, Sun R, Damania B. Characterization of Kaposi's sarcoma-associated herpesvirus (KSHV) K1 promoter activation by Rta. *Virology.* 2006;348(2):309-27. Epub 2006/03/21. doi: 10.1016/j.virol.2006.02.007. PubMed PMID: 16546233.
74. Sathish N, Yuan Y. Functional characterization of Kaposi's sarcoma-associated herpesvirus small capsid protein by bacterial artificial chromosome-based mutagenesis. *Virology.* 2010;407(2):306-18. Epub 2010/09/21. doi: 10.1016/j.virol.2010.08.017. PubMed PMID: 20850163.
75. Majerciak V, Yamanegi K, Zheng ZM. Gene structure and expression of Kaposi's sarcoma-associated herpesvirus ORF56, ORF57, ORF58, and ORF59. *J Virol.* 2006;80(24):11968-81. doi: 10.1128/JVI.01394-06. PubMed PMID: 17020939; PMCID: 1676266.
76. Kronstad LM, Brulois KF, Jung JU, Glaunsinger BA. Reinitiation after translation of two upstream open reading frames (ORF) governs expression of the ORF35-37 Kaposi's sarcoma-associated herpesvirus polycistronic mRNA. *J Virol.* 2014;88(11):6512-8. Epub 2014/03/14. doi: 10.1128/JVI.00202-14. PubMed PMID: 24623444; PMCID: PMC4093840.
77. Chung YH, Means RE, Choi JK, Lee BS, Jung JU. Kaposi's sarcoma-associated herpesvirus OX2 glycoprotein activates myeloid-lineage cells to induce inflammatory cytokine production. *J Virol.* 2002;76(10):4688-98. Epub 2002/04/23. PubMed PMID: 11967286; PMCID: PMC136121.

78. Rossetto CC, Pari GS. PAN's Labyrinth: Molecular biology of Kaposi's sarcoma-associated herpesvirus (KSHV) PAN RNA, a multifunctional long noncoding RNA. *Viruses*. 2014;6(11):4212-26. doi: 10.3390/v6114212. PubMed PMID: 25375885; PMCID: PMC4246217.
79. Lukac DM, Garibyan L, Kirshner JR, Palmeri D, Ganem D. DNA binding by Kaposi's sarcoma-associated herpesvirus lytic switch protein is necessary for transcriptional activation of two viral delayed early promoters. *J Virol*. 2001;75(15):6786-99. Epub 2001/07/04. doi: 10.1128/JVI.75.15.6786-6799.2001. PubMed PMID: 11435557; PMCID: PMC114405.
80. Xu Y, AuCoin DP, Huete AR, Cei SA, Hanson LJ, Pari GS. A Kaposi's sarcoma-associated herpesvirus/human herpesvirus 8 ORF50 deletion mutant is defective for reactivation of latent virus and DNA replication. *J Virol*. 2005;79(6):3479-87. Epub 2005/02/26. doi: 10.1128/JVI.79.6.3479-3487.2005. PubMed PMID: 15731242; PMCID: PMC1075731.
81. Lukac DM, Renne R, Kirshner JR, Ganem D. Reactivation of Kaposi's sarcoma-associated herpesvirus infection from latency by expression of the ORF 50 transactivator, a homolog of the EBV R protein. *Virology*. 1998;252(2):304-12. Epub 1999/01/08. doi: 10.1006/viro.1998.9486. PubMed PMID: 9878608.
82. Wang Y, Tang Q, Maul GG, Yuan Y. Kaposi's sarcoma-associated herpesvirus ori-Lyt-dependent DNA replication: dual role of replication and transcription activator. *J Virol*. 2006;80(24):12171-86. Epub 2006/10/06. doi: 10.1128/JVI.00990-06. PubMed PMID: 17020951; PMCID: PMC1676287.
83. Wang SE, Wu FY, Fujimuro M, Zong J, Hayward SD, Hayward GS. Role of CCAAT/enhancer-binding protein alpha (C/EBPalpha) in activation of the Kaposi's sarcoma-associated herpesvirus (KSHV) lytic-cycle replication-associated protein (RAP) promoter in cooperation with the KSHV replication and transcription activator (RTA) and RAP. *J Virol*. 2003;77(1):600-23. Epub 2002/12/13. PubMed PMID: 12477864; PMCID: PMC140597.
84. Lan K, Kuppers DA, Robertson ES. Kaposi's sarcoma-associated herpesvirus reactivation is regulated by interaction of latency-associated nuclear antigen with recombination signal sequence-binding protein Jkappa, the major downstream effector of the Notch signaling pathway. *J Virol*. 2005;79(6):3468-78. Epub 2005/02/26. doi: 10.1128/JVI.79.6.3468-3478.2005. PubMed PMID: 15731241; PMCID: PMC1075732.
85. Li Q, Zhou F, Ye F, Gao SJ. Genetic disruption of KSHV major latent nuclear antigen LANA enhances viral lytic transcriptional program. *Virology*. 2008;379(2):234-44. Epub 2008/08/08. doi: 10.1016/j.virol.2008.06.043. PubMed PMID: 18684478; PMCID: PMC2626151.
86. Lu F, Day L, Gao SJ, Lieberman PM. Acetylation of the latency-associated nuclear antigen regulates repression of Kaposi's sarcoma-associated herpesvirus lytic transcription. *J Virol*. 2006;80(11):5273-82. Epub 2006/05/16. doi: 10.1128/JVI.02541-05. PubMed PMID: 16699007; PMCID: PMC1472144.

87. Chen L, Lagunoff M. Establishment and maintenance of Kaposi's sarcoma-associated herpesvirus latency in B cells. *J Virol.* 2005;79(22):14383-91. doi: 10.1128/JVI.79.22.14383-14391.2005. PubMed PMID: 16254372; PMCID: 1280215.
88. Chan SR, Chandran B. Characterization of human herpesvirus 8 ORF59 protein (PF-8) and mapping of the processivity and viral DNA polymerase-interacting domains. *J Virol.* 2000;74(23):10920-9. PubMed PMID: 11069986; PMCID: 113171.
89. Chen Y, Ciustea M, Ricciardi RP. Processivity factor of KSHV contains a nuclear localization signal and binding domains for transporting viral DNA polymerase into the nucleus. *Virology.* 2005;340(2):183-91. doi: 10.1016/j.virol.2005.06.017. PubMed PMID: 16043206.
90. Lin K, Dai CY, Ricciardi RP. Cloning and functional analysis of Kaposi's sarcoma-associated herpesvirus DNA polymerase and its processivity factor. *J Virol.* 1998;72(7):6228-32. PubMed PMID: 9621095; PMCID: 110445.
91. AuCoin DP, Colletti KS, Cei SA, Papouskova I, Tarrant M, Pari GS. Amplification of the Kaposi's sarcoma-associated herpesvirus/human herpesvirus 8 lytic origin of DNA replication is dependent upon a cis-acting AT-rich region and an ORF50 response element and the trans-acting factors ORF50 (K-Rta) and K8 (K-bZIP). *Virology.* 2004;318(2):542-55. doi: 10.1016/j.virol.2003.10.016. PubMed PMID: 14972523.
92. Cheong WC, Park JH, Kang HR, Song MJ. Downregulation of Poly(ADP-Ribose) Polymerase 1 by a Viral Processivity Factor Facilitates Lytic Replication of Gammaherpesvirus. *J Virol.* 2015;89(18):9676-82. doi: 10.1128/JVI.00559-15. PubMed PMID: 26157130; PMCID: 4542354.
93. Di Domenico EG, Toma L, Bordignon V, Trento E, D'Agosto G, Cordiali-Fei P, Ensoli F. Activation of DNA Damage Response Induced by the Kaposi's Sarcoma-Associated Herpes Virus. *Int J Mol Sci.* 2016;17(6). doi: 10.3390/ijms17060854. PubMed PMID: 27258263; PMCID: 4926388.
94. Strahan RC, McDowell-Sargent M, Uppal T, Purushothaman P, Verma SC. KSHV encoded ORF59 modulates histone arginine methylation of the viral genome to promote viral reactivation. *PLoS Pathog.* 2017;13(7):e1006482. doi: 10.1371/journal.ppat.1006482. PubMed PMID: 28678843; PMCID: PMC5513536.
95. Borer RA, Lehner CF, Eppenberger HM, Nigg EA. Major nucleolar proteins shuttle between nucleus and cytoplasm. *Cell.* 1989;56(3):379-90. PubMed PMID: 2914325.
96. Ginisty H, Sicard H, Roger B, Bouvet P. Structure and functions of nucleolin. *J Cell Sci.* 1999;112 (Pt 6):761-72. PubMed PMID: 10036227.
97. Salvetti A, Coute Y, Epstein A, Arata L, Kraut A, Navratil V, Bouvet P, Greco A. Nuclear Functions of Nucleolin through Global Proteomics and Interactomic Approaches. *J Proteome Res.* 2016;15(5):1659-69. doi: 10.1021/acs.jproteome.6b00126. PubMed PMID: 27049334.
98. Tajrishi MM, Tuteja R, Tuteja N. Nucleolin: The most abundant multifunctional phosphoprotein of nucleolus. *Commun Integr Biol.* 2011;4(3):267-75. doi: 10.4161/cib.4.3.14884. PubMed PMID: 21980556; PMCID: 3187884.

99. Forsburg SL. Eukaryotic MCM proteins: beyond replication initiation. *Microbiol Mol Biol Rev.* 2004;68(1):109-31. PubMed PMID: 15007098; PMCID: PMC362110.
100. Bailis JM, Forsburg SL. MCM proteins: DNA damage, mutagenesis and repair. *Curr Opin Genet Dev.* 2004;14(1):17-21. doi: 10.1016/j.gde.2003.11.002. PubMed PMID: 15108800.
101. Majerciak V, Pripuzova N, Chan C, Temkin N, Specht SI, Zheng ZM. Stability of structured Kaposi's sarcoma-associated herpesvirus ORF57 protein is regulated by protein phosphorylation and homodimerization. *J Virol.* 2015;89(6):3256-74. doi: 10.1128/JVI.03721-14. PubMed PMID: 25568207; PMCID: PMC4337553.
102. Majerciak V, Uranishi H, Kruhlak M, Pilkington GR, Massimelli MJ, Bear J, Pavlakis GN, Felber BK, Zheng ZM. Kaposi's sarcoma-associated herpesvirus ORF57 interacts with cellular RNA export cofactors RBM15 and OTT3 to promote expression of viral ORF59. *J Virol.* 2011;85(4):1528-40. doi: 10.1128/JVI.01709-10. PubMed PMID: 21106733; PMCID: 3028919.
103. Bugler B, Bourbon H, Lapeyre B, Wallace MO, Chang JH, Amalric F, Olson MO. RNA binding fragments from nucleolin contain the ribonucleoprotein consensus sequence. *J Biol Chem.* 1987;262(23):10922-5. PubMed PMID: 2440879.
104. Orrick LR, Olson MO, Busch H. Comparison of nucleolar proteins of normal rat liver and Novikoff hepatoma ascites cells by two-dimensional polyacrylamide gel electrophoresis. *Proc Natl Acad Sci U S A.* 1973;70(5):1316-20. PubMed PMID: 4351171; PMCID: PMC433487.
105. Lei M. The MCM complex: its role in DNA replication and implications for cancer therapy. *Curr Cancer Drug Targets.* 2005;5(5):365-80. PubMed PMID: 16101384.
106. Chan SR, Bloomer C, Chandran B. Identification and characterization of human herpesvirus-8 lytic cycle-associated ORF 59 protein and the encoding cDNA by monoclonal antibody. *Virology.* 1998;240(1):118-26. Epub 1998/02/04. doi: 10.1006/viro.1997.8911. PubMed PMID: 9448696.
107. Chen X, Lin K, Ricciardi RP. Human Kaposi's sarcoma herpesvirus processivity factor-8 functions as a dimer in DNA synthesis. *J Biol Chem.* 2004;279(27):28375-86. Epub 2004/04/13. doi: 10.1074/jbc.M400032200. PubMed PMID: 15075322.
108. Neipel F, Albrecht JC, Fleckenstein B. Cell-homologous genes in the Kaposi's sarcoma-associated rhadinovirus human herpesvirus 8: determinants of its pathogenicity? *J Virol.* 1997;71(6):4187-92. Epub 1997/06/01. PubMed PMID: 9151804; PMCID: PMC191632.
109. Majerciak V, Zheng ZM. KSHV ORF57, a protein of many faces. *Viruses.* 2015;7(2):604-33. doi: 10.3390/v7020604. PubMed PMID: 25674768; PMCID: 4353906.
110. Ma Y, Liu P, Majerciak V, Zhu J, Zheng ZM. CLIP-seq to Identify KSHV ORF57-Binding RNA in Host B Cells. *Curr Protoc Microbiol.* 2016;41:1E 11 1-1E 8. doi: 10.1002/cpmc.3. PubMed PMID: 27153386.

111. Vogt C, Bohne J. The KSHV RNA regulator ORF57: target specificity and its role in the viral life cycle. *Wiley Interdiscip Rev RNA*. 2016;7(2):173-85. Epub 2016/01/16. doi: 10.1002/wrna.1323. PubMed PMID: 26769399.
112. Jackson BR, Boyne JR, Noerenberg M, Taylor A, Hautbergue GM, Walsh MJ, Wheat R, Blackbourn DJ, Wilson SA, Whitehouse A. An interaction between KSHV ORF57 and UIF provides mRNA-adaptor redundancy in herpesvirus intronless mRNA export. *PLoS Pathog*. 2011;7(7):e1002138. Epub 2011/08/05. doi: 10.1371/journal.ppat.1002138. PubMed PMID: 21814512; PMCID: PMC3141038.
113. Hunter OV, Sei E, Richardson RB, Conrad NK. Chromatin immunoprecipitation and microarray analysis suggest functional cooperation between Kaposi's Sarcoma-associated herpesvirus ORF57 and K-bZIP. *J Virol*. 2013;87(7):4005-16. Epub 2013/02/01. doi: 10.1128/JVI.03459-12. PubMed PMID: 23365430; PMCID: PMC3624208.
114. Malik P, Blackbourn DJ, Clements JB. The evolutionarily conserved Kaposi's sarcoma-associated herpesvirus ORF57 protein interacts with REF protein and acts as an RNA export factor. *J Biol Chem*. 2004;279(31):33001-11. Epub 2004/05/25. doi: 10.1074/jbc.M313008200. PubMed PMID: 15155762.
115. Boyne JR, Whitehouse A. Nucleolar disruption impairs Kaposi's sarcoma-associated herpesvirus ORF57-mediated nuclear export of intronless viral mRNAs. *FEBS Lett*. 2009;583(22):3549-56. doi: 10.1016/j.febslet.2009.10.040. PubMed PMID: 19850040.
116. Nekorchuk M, Han Z, Hsieh TT, Swaminathan S. Kaposi's sarcoma-associated herpesvirus ORF57 protein enhances mRNA accumulation independently of effects on nuclear RNA export. *J Virol*. 2007;81(18):9990-8. Epub 2007/07/05. doi: 10.1128/JVI.00896-07. PubMed PMID: 17609285; PMCID: PMC2045429.
117. Pilkington GR, Majerciak V, Bear J, Uranishi H, Zheng ZM, Felber BK. Kaposi's sarcoma-associated herpesvirus ORF57 is not a bona fide export factor. *J Virol*. 2012;86(23):13089-94. Epub 2012/09/21. doi: 10.1128/JVI.00606-12. PubMed PMID: 22993146; PMCID: PMC3497679.
118. Kang JG, Pripuzova N, Majerciak V, Kruhlak M, Le SY, Zheng ZM. Kaposi's sarcoma-associated herpesvirus ORF57 promotes escape of viral and human interleukin-6 from microRNA-mediated suppression. *J Virol*. 2011;85(6):2620-30. doi: 10.1128/JVI.02144-10. PubMed PMID: 21209110; PMCID: 3067933.
119. Massimelli MJ, Majerciak V, Kruhlak M, Zheng ZM. Interplay between polyadenylate-binding protein 1 and Kaposi's sarcoma-associated herpesvirus ORF57 in accumulation of polyadenylated nuclear RNA, a viral long noncoding RNA. *J Virol*. 2013;87(1):243-56. doi: 10.1128/JVI.01693-12. PubMed PMID: 23077296; PMCID: 3536381.
120. Palmeri D, Spadavecchia S, Carroll KD, Lukac DM. Promoter- and cell-specific transcriptional transactivation by the Kaposi's sarcoma-associated herpesvirus ORF57/Mta protein. *J Virol*. 2007;81(24):13299-314. Epub 2007/10/05. doi: 10.1128/JVI.00732-07. PubMed PMID: 17913801; PMCID: PMC2168867.
121. Majerciak V, Deng M, Zheng ZM. Requirement of UAP56, URH49, RBM15, and OTT3 in the expression of Kaposi sarcoma-associated herpesvirus ORF57. *Virology*.

- 2010;407(2):206-12. doi: 10.1016/j.virol.2010.08.014. PubMed PMID: 20828777; PMCID: 2952739.
122. Sahin BB, Patel D, Conrad NK. Kaposi's sarcoma-associated herpesvirus ORF57 protein binds and protects a nuclear noncoding RNA from cellular RNA decay pathways. *PLoS Pathog.* 2010;6(3):e1000799. Epub 2010/03/12. doi: 10.1371/journal.ppat.1000799. PubMed PMID: 20221435; PMCID: PMC2832700.
123. Verma D, Li DJ, Krueger B, Renne R, Swaminathan S. Identification of the physiological gene targets of the essential lytic replicative Kaposi's sarcoma-associated herpesvirus ORF57 protein. *J Virol.* 2015;89(3):1688-702. doi: 10.1128/JVI.02663-14. PubMed PMID: 25410858; PMCID: PMC4300733.
124. Majerciak V, Yamanegi K, Allemand E, Kruhlik M, Krainer AR, Zheng ZM. Kaposi's sarcoma-associated herpesvirus ORF57 functions as a viral splicing factor and promotes expression of intron-containing viral lytic genes in spliceosome-mediated RNA splicing. *J Virol.* 2008;82(6):2792-801. doi: 10.1128/JVI.01856-07. PubMed PMID: 18184716; PMCID: 2258979.
125. Kirshner JR, Lukac DM, Chang J, Ganem D. Kaposi's sarcoma-associated herpesvirus open reading frame 57 encodes a posttranscriptional regulator with multiple distinct activities. *J Virol.* 2000;74(8):3586-97. PubMed PMID: 10729134; PMCID: PMC111868.
126. Massimelli MJ, Majerciak V, Kang JG, Liewehr DJ, Steinberg SM, Zheng ZM. Multiple regions of Kaposi's sarcoma-associated herpesvirus ORF59 RNA are required for its expression mediated by viral ORF57 and cellular RBM15. *Viruses.* 2015;7(2):496-510. doi: 10.3390/v7020496. PubMed PMID: 25690794; PMCID: 4353900.
127. Massimelli MJ, Kang JG, Majerciak V, Le SY, Liewehr DJ, Steinberg SM, Zheng ZM. Stability of a long noncoding viral RNA depends on a 9-nt core element at the RNA 5' end to interact with viral ORF57 and cellular PABPC1. *Int J Biol Sci.* 2011;7(8):1145-60. PubMed PMID: 22043172; PMCID: 3204405.
128. Conrad NK. New insights into the expression and functions of the Kaposi's sarcoma-associated herpesvirus long noncoding PAN RNA. *Virus Res.* 2016;212:53-63. Epub 2015/06/24. doi: 10.1016/j.virusres.2015.06.012. PubMed PMID: 26103097; PMCID: PMC4686379.
129. Rossetto CC, Pari GS. Kaposi's sarcoma-associated herpesvirus noncoding polyadenylated nuclear RNA interacts with virus- and host cell-encoded proteins and suppresses expression of genes involved in immune modulation. *J Virol.* 2011;85(24):13290-7. Epub 2011/10/01. doi: 10.1128/JVI.05886-11. PubMed PMID: 21957289; PMCID: PMC3233155.
130. Srivastava M, Pollard HB. Molecular dissection of nucleolin's role in growth and cell proliferation: new insights. *FASEB J.* 1999;13(14):1911-22. Epub 1999/11/02. PubMed PMID: 10544174.
131. Bender BJ, Coen DM, Strang BL. Dynamic and nucleolin-dependent localization of human cytomegalovirus UL84 to the periphery of viral replication compartments and nucleoli. *J Virol.* 2014;88(20):11738-47. doi: 10.1128/JVI.01889-14. PubMed PMID: 25078694; PMCID: 4178712.

132. Calle A, Ugrinova I, Epstein AL, Bouvet P, Diaz JJ, Greco A. Nucleolin is required for an efficient herpes simplex virus type 1 infection. *J Virol*. 2008;82(10):4762-73. Epub 2008/03/07. doi: 10.1128/JVI.00077-08. PubMed PMID: 18321972; PMCID: PMC2346767.
133. Chen YL, Liu CD, Cheng CP, Zhao B, Hsu HJ, Shen CL, Chiu SJ, Kieff E, Peng CW. Nucleolin is important for Epstein-Barr virus nuclear antigen 1-mediated episome binding, maintenance, and transcription. *Proc Natl Acad Sci U S A*. 2014;111(1):243-8. doi: 10.1073/pnas.1321800111. PubMed PMID: 24344309; PMCID: PMC3890893.
134. Greco A, Arata L, Soler E, Gaume X, Coute Y, Hacot S, Calle A, Monier K, Epstein AL, Sanchez JC, Bouvet P, Diaz JJ. Nucleolin interacts with US11 protein of herpes simplex virus 1 and is involved in its trafficking. *J Virol*. 2012;86(3):1449-57. Epub 2011/12/02. doi: 10.1128/JVI.06194-11. PubMed PMID: 22130536; PMCID: PMC3264372.
135. Strang BL, Boulant S, Coen DM. Nucleolin associates with the human cytomegalovirus DNA polymerase accessory subunit UL44 and is necessary for efficient viral replication. *J Virol*. 2010;84(4):1771-84. doi: 10.1128/JVI.01510-09. PubMed PMID: 20007282; PMCID: 2812382.
136. Muller M, Hutin S, Marigold O, Li KH, Burlingame A, Glaunsinger BA. A ribonucleoprotein complex protects the interleukin-6 mRNA from degradation by distinct herpesviral endonucleases. *PLoS Pathog*. 2015;11(5):e1004899. doi: 10.1371/journal.ppat.1004899. PubMed PMID: 25965334; PMCID: 4428876.
137. Strang BL, Boulant S, Kirchhausen T, Coen DM. Host cell nucleolin is required to maintain the architecture of human cytomegalovirus replication compartments. *MBio*. 2012;3(1). doi: 10.1128/mBio.00301-11. PubMed PMID: 22318319; PMCID: 3280463.
138. Han Z, Swaminathan S. Kaposi's sarcoma-associated herpesvirus lytic gene ORF57 is essential for infectious virion production. *J Virol*. 2006;80(11):5251-60. Epub 2006/05/16. doi: 10.1128/JVI.02570-05. PubMed PMID: 16699005; PMCID: PMC1472138.
139. Boyne JR, Jackson BR, Taylor A, Macnab SA, Whitehouse A. Kaposi's sarcoma-associated herpesvirus ORF57 protein interacts with PYM to enhance translation of viral intronless mRNAs. *EMBO J*. 2010;29(11):1851-64. doi: 10.1038/emboj.2010.77. PubMed PMID: 20436455; PMCID: PMC2885933.
140. Lista MJ, Martins RP, Billant O, Contesse MA, Findakly S, Pochard P, Daskalogianni C, Beauvineau C, Guetta C, Jamin C, Teulade-Fichou MP, Fahraeus R, Voisset C, Blondel M. Nucleolin directly mediates Epstein-Barr virus immune evasion through binding to G-quadruplexes of EBNA1 mRNA. *Nat Commun*. 2017;8:16043. Epub 2017/07/08. doi: 10.1038/ncomms16043. PubMed PMID: 28685753; PMCID: PMC5504353.
141. Tsuyama T, Tada S, Watanabe S, Seki M, Enomoto T. Licensing for DNA replication requires a strict sequential assembly of Cdc6 and Cdt1 onto chromatin in *Xenopus* egg extracts. *Nucleic Acids Res*. 2005;33(2):765-75. Epub 2005/02/03. doi: 10.1093/nar/gki226. PubMed PMID: 15687385; PMCID: PMC548366.

142. Stedman W, Deng Z, Lu F, Lieberman PM. ORC, MCM, and histone hyperacetylation at the Kaposi's sarcoma-associated herpesvirus latent replication origin. *J Virol.* 2004;78(22):12566-75. Epub 2004/10/28. doi: 10.1128/JVI.78.22.12566-12575.2004. PubMed PMID: 15507644; PMCID: PMC525046.
143. Wiebusch L, Uecker R, Hagemeyer C. Human cytomegalovirus prevents replication licensing by inhibiting MCM loading onto chromatin. *EMBO Rep.* 2003;4(1):42-6. doi: 10.1038/sj.embor.embor707. PubMed PMID: 12524519; PMCID: PMC1315807.
144. Kudoh A, Daikoku T, Ishimi Y, Kawaguchi Y, Shirata N, Iwahori S, Isomura H, Tsurumi T. Phosphorylation of MCM4 at sites inactivating DNA helicase activity of the MCM4-MCM6-MCM7 complex during Epstein-Barr virus productive replication. *J Virol.* 2006;80(20):10064-72. doi: 10.1128/JVI.00678-06. PubMed PMID: 17005684; PMCID: PMC1617282.
145. Caizergues-Ferrer M, Belenguer P, Lapeyre B, Amalric F, Wallace MO, Olson MO. Phosphorylation of nucleolin by a nucleolar type NII protein kinase. *Biochemistry.* 1987;26(24):7876-83. Epub 1987/12/01. PubMed PMID: 3427111.
146. Zhou G, Seibenhener ML, Wooten MW. Nucleolin is a protein kinase C-zeta substrate. Connection between cell surface signaling and nucleus in PC12 cells. *J Biol Chem.* 1997;272(49):31130-7. Epub 1998/01/10. PubMed PMID: 9388266.
147. Dranovsky A, Vincent I, Gregori L, Schwarzman A, Colflesh D, Enghild J, Strittmatter W, Davies P, Goldgaber D. Cdc2 phosphorylation of nucleolin demarcates mitotic stages and Alzheimer's disease pathology. *Neurobiol Aging.* 2001;22(4):517-28. Epub 2001/07/11. PubMed PMID: 11445251.
148. Yang C, Maignel DA, Carrier F. Identification of nucleolin and nucleophosmin as genotoxic stress-responsive RNA-binding proteins. *Nucleic Acids Res.* 2002;30(10):2251-60. Epub 2002/05/10. PubMed PMID: 12000845; PMCID: PMC115285.